5-2016

Tractor Measurement and Data Acquisition System for Hydraulic Power, Draft Force, and Power Take-off Torque

James Roeber
University of Nebraska - Lincoln, roeber.james90@huskers.unl.edu

TRACTOR MEASUREMENT AND DATA ACQUISITION SYSTEM FOR HYDRAULIC POWER, DRAFT FORCE, AND POWER TAKE-OFF TORQUE

by

James B. W. Roeber

A THESIS

Presented to the Faculty of

The Graduate College at the University of Nebraska

In Partial Fulfillment of Requirements

For the Degree of Master of Science

Major: Agricultural and Biological Systems Engineering

Under the Supervision of
Professor Santosh K. Pitla
&
Professor Roger M. Hoy

Lincoln, Nebraska

May, 2016

TRACTOR MEASUREMENT AND DATA ACQUISITION SYSTEM FOR HYDRAULIC POWER, DRAFT FORCE, AND POWER TAKE-OFF TORQUE

James B. W. Roeber, M.S.

University of Nebraska, 2016

Advisor: Santosh K. Pitla and Roger M. Hoy

Numerous advancements in machinery performance of agricultural tractors have been made in recent years. The Organisation for Economic Co-operation and Development (OECD) tests predetermined points (e.g., maximum power and torque) for drawbar, Power Take-Off (PTO), and hydraulic power as separate tests for tractor performance. Testing methods with the tractor operating at a steady state have been done for years, which were uncharacteristic of agricultural tractor operations in field conditions. As part of this thesis work, field usable data acquisition systems (DAQs) were developed to record implement energy consumption (e.g., drawbar loading, PTO torque, and hydraulic power). The system used LabVIEW software and National Instrument's compact data acquisition systems (cDAQs) to record data from instrumentation measuring drawbar, PTO, and hydraulic loads. Data were collected and verified in accordance with OECD standards at the Nebraska Tractor Test Lab (NTTL), an official OECD testing facility. Requirements of the systems were: implementation of each system on multiple machines with minor alterations, minimal changes to the tractor, and equivalent data compared to that recorded by the NTTL testing devices and procedures. Manufacturer's calibration information along with standardized testing equipment used to tune NTTL testing devices were used to verify that the system would provide data in

conformance with OECD testing procedures. The hydraulic system was verified with varying hydraulic line curvatures near the sensors that provided data within a 1 percent difference of the actual hydraulic power. Drawbar tests included calibration of a strain gage instrumented drawbar which recorded loads within 0.67 kN of the calibration fixture. Track testing of the drawbar resulted in measured differences of less than 1 kN with the NTTL load car. For PTO measurements, a power take-off calibration was conducted using a commercially available torque transducer. No statistically significant differences were found between the torque values of the PTO transducer and the dynamometer. The differences in torque values ranged from 3 N·m to 23 N·m.

Acknowledgments

I would like to thank my advisor, Dr. Santosh Pitla. For without his knowledge and guidance, none of this would have been possible. He has been a great mentor over the past 3 years, and I continue to appreciate all he has done for me. I would also like to thank my committee members, Roger Hoy, Joe Luck, and Mike Kocher, for all their support and direction.

To Doug Triplett, Rodney Rohrer, Justin Geyer, and Brent Sampson, I would like to extend thanks for all the assistance and knowledge involved in LabVIEW, OECD Code 2, and NTTL tractor test procedures. Thank you to all the undergraduate student workers of the NTTL who helped with test setup and operation of the tractor during tests.

I would like to thank my family and friends for all their support in my decision to further my education. My parents, Kim and Bruce, have always been supportive in my pursuit of education and have always been willing to help me reach my goals.

Finally, I would like to thank the Lord for providing me with the ability to do His work, and to give me the strength to overcome the obstacles in my path. For it is He who makes all things possible.

TABLE OF CONTENTS

FIGURES

TABLES

Chapter 1 INTRODUCTION

1.1 INTRODUCTION

Agricultural tractors are used throughout the year for various operations, utilizing different implements. Tractors deliver power to implements via draft, hydraulic, and PTO power. Several of these operations require at least two forms of tractor power, either continuous power from the tractor (e.g. drawbar, PTO), or intermittent operations (e.g. hydraulics).

Tractor performance is measured according to the standards of The Organisation for Economic Co-operation and Development (OECD) Code 2 for the official testing of agricultural and forestry tractor performance. All OECD approved tractors must complete a set of tests to determine tractor performance through the PTO, tractive performance as a result of drawbar draft force, and hydraulic power as separate tests. (OECD, 2016). The advent of electronically controlled engines have resulted in tractors that deliver different engine performance based on which power outlets are being utilized. Examples of these varying power curves are found on the Case IH Magnum 380 which can run in an increased power mode at certain combinations of drawbar loading and remote hydraulic flow. Late-model Case IH Steiger wheeled, Steiger Quadtrac/Rowtrac track-laying tractors, and current John Deere 9R models limit the power in select gears to protect the drivetrain (NTTL, 2014; NTTL, 2015; NTTL, 2016).

The mandatory test for hydraulic power required the hydraulic case fluid to be within a 5 degree tolerance of 65°C, and was to be stated in the report if control of temperature within this range could not be achieved. In normal operating conditions,

environmental temperature and operating load can have an effect on the initial and rate of change of the fluid temperature. The test must also be conducted with engine at maximum speed and flow controls adjusted to achieve maximum flow, which is not always reasonable for normal operations.

Similarly, when testing drawbar performance, tractors are tested in the gear/speed setting immediately above the gear/speed setting producing maximum power down to the gear/speed setting immediately below the gear/speed setting producing maximum pull. However, the fuel consumption test during the drawbar power test (section 4.4.2.2, OECD 2016) provides information on operational efficiency at partial loads. This section of the test consists of five sub tests: maximum drawbar power at rated engine speed (RES), two tests that are at 50 per cent, and two tests at 75 per cent of pull at maximum drawbar power at RES. Travel speed in the selected gears must be the same at each load, with one gear/speed setting at RES, and the other in a higher gear and reduced engine speed. These tests are performed to assess two gear/speed settings typically used for fieldwork, and the OECD Code 2 requires one be a gear/speed setting that results in the travel speed as close to a nominal speed of 7.5 $km \cdot h^{-1}$ and the other gear/speed setting be one that results in a nominal travel speed between 7 and 10 $km \cdot h^{-1}$. The Nebraska Tractor Test Board Action No. 6 requires that the maximum drawbar power shall be determined:

a. in all gears which produce less than 15% slip and a speed of less than 12.9 $km \cdot h^{-1}$ (8 mph) at rated engine speed,
b. the gear below the slowest run from part a with the load adjusted to produce slip near 15%, and
c. a gear producing a speed between 12.9 and 16.1 $km \cdot h^{-1}$ (8 and 10 mph) at rated

engine speed (NTTL, 1998).

Power Take-off test sections require the maximum governor setting. The tests proceed to test the maximum power for a period of one hour (section 4.1.1.1, OECD 2016), full load at varying speed (section 4.1.1.2, OECD 2016), varying load at rated engine speed and at standard PTO speed (section 4.1.1.3, OECD 2016). Fuel consumption tests exist to establish engine fuel use characteristics, enabling evaluation of the PTO operation fuel economy (section 4.1.3, OECD 2016). The test parameters include:

1. maximum power at RES;
2. heavy drawbar work (80 % RES maximum power at maximum speed setting);
3. heavy drawbar power or PTO at standard speed
   (80 % RES maximum power with governor set to 90 % RES);
4. light PTO power or drawbar (40 % RES maximum power set to 90 % RES);
5. heavy drawbar or PTO at economy PTO speeds or automatic engine speed control
   (60 % RES maximum power with governor set to 60 % RES);
6. light drawbar or PTO at reduced speed (40 % RES maximum power with
   governor set to 60 % RES).

Additional tests are included to measure PTOs that are designed to provide standard PTO speed at lower engine speeds (section 4.1.3.2, OECD 2016). The tests require maximum power to be measured at a speed equivalent to rated engine speed and at the engine speed giving standard PTO speed. Tractors unable to transmit full power of the engine through the PTO are tested under the type of coupling between the engine and the PTO, mechanical or non-mechanical coupling (section 4.1.4, OECD 2016). A mechanical

coupling test will consist of a two-hour test at maximum power. Torque must be increased 20 per cent every five minutes for a period of no more than 60 seconds. Non-mechanical coupling tests include a two-hour test consisting of 2 separate one-hour tests sequentially and a series of tests at part loads. The first hour-test maximum power reported will be the average of a minimum number of six readings spaced evenly throughout the hour. The second one-hour test will be at the lowest engine speed which will maintain the PTO power from the first one-hour test at rated PTO speed. Power Take-off at part loads are completed with the governor control as set for the second one-hour test. These loads must last 20 minutes minimally and be made according to the main PTO varying loads at RES.

1.2 REVIEW OF LITERATURE

Most implements are not used in a steady state for fieldwork and utilize more than one source of power transfer between the tractor and the implement during operation. Current testing procedures at the OECD-approved Nebraska Tractor Test Laboratory (NTTL) do not measure multiple power flows simultaneously. A new tractor testing methodology referred to as PowerMix testing was used in Germany at the Deutsche Landwirtschafts Gesellschaft (DLG) Test Center Technology and Farm Inputs (Lech & Winter, 2015). The DLG PowerMix test was a first attempt at a mixed power mode test but imposed load profiles based on a small tractor working in Germany and therefore applicability of the test to other size tractors in other markets was questionable. The primary PowerMix testing objective was to document fuel use characteristics under field and transport operations and perform the PowerMix test by combining traction, PTO, and

hydraulic loads while measuring the specific fuel consumption under fourteen different workload scenarios. Implements included in the scenarios: plough, cultivator, rotary harrow, mower, manure spreader, and baler. Drawbar work (plough, cultivator) are loaded to 60 and 100 per cent test cycles, and the drawbar/PTO (harrow, mower) utilized 40, 60, and 100 per cent test cycles (Lech & Winter, 2015).

One of the most frequently used standards for agricultural machinery is the ASAE Standard D497.7 Agricultural Machinery Management (ASABE Standards, 2011). This standard gave information on required implement draft power, PTO power, and operating speeds. Differences in machine design, machine adjustment, machine condition, and crop characteristics are accounted for by the expected range value which can vary from 15 to 50 percent of the typical value. This could significantly affect the proper sizing of machinery combinations.

Research of implement power requirements has been conducted to study the power output of a single tractor performing several operations. Direction of travel affected the required power of a tandem disk after plowing. Traveling parallel to the plowing direction, the power requirement was steady within 3.7 kW (~5 HP); however, perpendicular travel caused greater fluctuations (12.5 kW). Heavy work operations varied from 56 to 97 percent of the maximum available tractor power (Ricketts and Weber, 1961). McLaughlin et.al. (2008) performed research using eight tillage implements in clay loam soil over a four year period. A Case International tractor (7110, J.I. Case Company, Racine, Wisc) was utilized for the tests. Power values ranged from 26.4 to 81.4 percent of the maximum available tractor power (McLaughlin et. al., 2008). The authors determined the agricultural machinery management equation for draft force

overestimated the moldboard plow, chisel plow and fluted coulter by 12 to 69 percent. Deep zone till, chisel sweep, and the disk harrow measured forces were underestimated by 24 to 36 percent. ASABE coefficients ranged from ±25 percent to ±50 percent for these implements.

If data were more readily available to show power requirements for the common types of implements for which tractors of a particular power class are typically used; the NTTL could incorporate additional test procedures for tractors used in the United States and other regions. Such tests could incorporate tests for tractors under multiple load conditions (i.e., PTO, hydraulic, and drawbar loads) to determine the performance and fuel use which a range of tractors sized similarly will experience in the field. Determining the appropriate load conditions requires current typical field operations to be monitored and standardized for a range of implement sizes and styles for a tractor appropriately chosen to provide power to those implements. The collected data could then be utilized to update the agricultural machinery management standard. Such data could also be used to continually develop a more realistic mixed power mode testing procedure for the NTTL and OECD.

Originally, a plan for measuring the implement interface was devised to log Controller Area Network (CANbus) data from the tractor. A channel list was created in accordance with the J1939 standard to gather messages from the bus. However, many of the desired message packets are not available publicly and another series of standards (ISO 11783, all parts) are required to properly interpret many of the implement/peripheral messages made available on the CANbus. A plan of this scale requires many hours of data analysis, post-processing, and limits the accuracy of the data collected due to the

inconsistency of CAN sampling rates. Further, not all tractors and implements are equipped with CANbus, therefore, a separate system would also be needed to ensure that relevant and accurate data from all tractors and implements are collected.

With the limited implement data that could be collected from the CANbus, attention shifted to other means of obtaining these data. Other researchers have used field operations with the intent to better understand and investigate tractor efficiencies. Burgun et al. (2013) instrumented a Massey Ferguson 6475 90kW tractor (a popular mid-sized tractor in France) for tillage, seeding, fertilizer, and transport operations, using embedded buses and sensors. Data was collected using the embedded buses (CAN and ISOBUS) and was then decoded using the SAE J1939 protocol to obtain engine speed ($rev \cdot min^{-1}$), engine percentage load (%), and fuel consumption (l/h) information. Additionally, global position data, vehicle speed, selected gear, and hitch position were collected using a dedicated recording device connected to the J1939 diagnostic plug available in the tractor cab. Burgun et al (2013), considered the three main power flows to be power delivered to the wheels (i.e., draft), the PTO, and the hydraulics. Torque meters and incremental encoders were used on both rear axles to measure each wheel's torque and speed independently. The purpose of measuring each wheel independently was due to a power differential in the axle housing that transferred power from the driveshaft to the axles, thus allowing the wheels to spin and transmit torque at different rates. Power delivered to the front wheels was obtained by measuring the torque and speed applied to the input of the front axle differential. The front axle speed was calculated from the known transmission ratio and the measured rear final drive differential speed. A commercially available PTO torque and speed sensor from DATUM was used for monitoring the power

delivered to an implement through the PTO shaft. The DATUM transducer is a contactless slip ring with a female coupler on one end and a male shaft on the other end. A flow turbine (HYDROTECHNIK RE6) and pressure transducer were installed in the main hydraulic pump line before the rear hydraulic remote connectors to determine the hydraulic power consumed. The authors failed to provide the exact location of the sensors between the main pump and hydraulic remote connectors. Any location before the hydraulic remote connectors would include the tractor hydraulic system inefficiencies. Other non-implement hydraulic loads the author's system had the potential to include were power steering operation, braking, and trailer brakes. Engine fan speed was recorded since a viscous fan drive was employed; which allowed the fan to rotate a different speed ratios when compared to engine speed. All the additional measured signals were connected to a CAMPBELL CR-3000 data acquisition board. The goal of Burgun et al. (2013) research was to evaluate agricultural machinery performance. This was done by documenting the power requirements of implements during field applications and in further developing a method to report the field efficiency (Burgun el al., 2013).

Other studies were done to measure and map the consumed energy and load states of implement operations in field conditions. A study by A. F. Kheiralla (2001) used a DAQ to map power and energy demand based on embedded tractor systems and custom-made sensors. A Massey Ferguson 3060 was selected as a representative tractor employed for general use on an oil palm plantation in Malaysia. The embedded system measured engine speed, PTO speed, forward speed, wheel slip, acres worked, fuel consumption per hour or hectare, acres per hour, cost factor, fuel consumed, fuel

remaining, and distance. This factory embedded system included a radar sensor for ground speed, a magnetic pickup to measure tractor rear wheel rotation, and a flow meter to measure fuel flow. Additional instrumentation included a custom-built drawbar transducer, wheel torque sensors, a PTO shaft torque sensor, and a 3-point lift mounted dynamometer. Drawbar force was measured with a proof ring installed toward the front of the drawbar to reduce lateral and longitudinal moments. An aluminum alloy was used to give the transducer greater sensitivity. Strain gages were bonded in pairs at the location the proof ring attached to the drawbar and at 90° locations on the inner and outer circumferences of the proof ring. The strain gages were wired in a full bridge configuration. The rear wheel torque transducers were designed based on extension shafts. A RBE-4A Kyowa slip ring and custom built adapters were applied to the axle and the tire rim. The PTO shaft torque transducer was a modified commercial drive shaft with a slip ring on the free female end and a universal joint on the other male end. A Data Electronics Datataker 605 along with a Compaq Contura 3/25C notebook was employed as the DAQ and used in-house Decipher Plus software (Kheiralla et al., 2001). Kheiralla did not present a method or measurement for measuring hydraulic power.

Pitla et al. (2014) used the embedded CANbus on a four-wheel drive tractor and a mechanical front wheel drive tractor to collect fuel rate, engine speed, and engine torque. The fuel rate data was used to determine the field efficiencies of an anhydrous applicator, cultivator, and planter. The authors concluded that use of the CANbus fuel rate data had the potential to predict field efficiencies of machines. A further extension of this research was to determine the load profile of the implements using the fuel rate (Pitla et al., 2016).

The authors concluded that load and fuel use rate data were able to determine the load profiles in a field.

1.3 OUTLINE OF RESEARCH

The research described in this thesis presents a different approach for the development of a data acquisition system to acquire agricultural implement power requirements during field operations. Subsystems were developed to interface with the single tractor power systems (i.e., hydraulic, drawbar, PTO) independently. To determine the necessary data to be collected, a signal list was established to represent the needed signals to measure draft loads (drawbar and 3-point), hydraulic power, and PTO shaft torque. The system was designed to be deployed on different tractor-implement combinations while minimizing alterations to the tractor and implement. Since a draft load would not be connected to both the drawbar and 3-point hitch simultaneously, measurement of draft loads connected to the drawbar was considered for the development of the system.

Chapter 2 summarizes the objectives of each data acquisition and measurement system developed as part of this research work. Chapters 3, 4, and 5 describe the development and verification of the individual data acquisition systems in detail. Each chapter is presented as a journal manuscript, suitable for independent publication.

Chapter 2 OBJECTIVES

The overall goal of this project was to develop portable measurement and data acquisition systems capable of measuring the implement load at the tractor/implement interface for hydraulic power, draft force, and PTO torque. Each of these systems were to be installed on a tractor with minimal alterations to the tractor. The independent systems were to be able to integrate with each other to create a comprehensive measurement and data acquisition system

2.1 HYDRAULIC POWER MEAUSREMENT SYSTEM OBJECTIVES

The goal of this project was to develop a portable hydraulic pressure and flow measurement system. This system would attach to the remote hydraulic ports at the rear of the tractor with minimal modifications to determine the hydraulic power delivered to an attached implement. Specific objectives of the current research work were to:

- Determine which of the six tubing configurations used with a portable hydraulic pressure and flow measurement system could be mounted without modification to a tractor and provide adjusted pressure and flow rate measurements with differences less than 2% and 0.5%, respectively.
- Determine whether the hydraulic power obtained using the portable hydraulic pressure and flow measurement system had differences less than 1% of full scale hydraulic measurement bench power measurement.

2.2 DRAW BAR DRAFT MEAUSREMENT SYSTEM OBJECTIVES

The goal of this project was to develop a portable draft measurement system. This system would measure the draft force applied by an implement on a tractor drawbar. Specific objectives were to:

- Calibrate the instrumented drawbar , and
- Use OECD Code 2 tractor drawbar power test procedures and the Nebraska Tractor Test Laboratory load car to determine if the difference in draft measurements between the instrumented drawbar and the load car were less than 2%.

2.3 POWER TAKE OFF TORQUE MEAUSREMENT SYSTEM OBJECTIVES

The goal of this project was to develop a portable PTO torque and rotational speed measurement system that can attach to the tractor with no modifications to the tractor PTO shaft. Specific objectives of the research work were to:

- Calibrate the PTO sensor using OECD Code 2 tractor PTO test at varying load procedures and the Nebraska Tractor Test Laboratory dynamometer for the torque transducer, and
- Use OECD Code 2 tractor PTO full load at varying speed test procedures and the Nebraska Tractor Test Laboratory dynamometer to determine if the sensor torque and power measurements were within 1% of the dynamometer.

Chapter 3 TRACTOR HYDRAULIC POWER DATA ACQUISITION SYSTEM

Abstract

Tractor hydraulic power is used on a wide range of agricultural implements; however, limited operational data at points other than maximum engine speed are generally available which operators could utilize to properly size machinery. A field usable hydraulic test apparatus capable of measuring tractor hydraulic pressure and flow rate data was developed. The goal of this study was to determine which of six hose configurations (necessary to install measurement devices for hydraulic pressure and flow rate in the space available at the rear of a tractor) provided measurement of hydraulic power delivered to attached implements within 2 % of the full hydraulic power available from the tractor. The measurement system installed allowed hydraulic hoses from the hydraulic remote ports to be attached to the flowmeter and pressure sensors with different bend angles in the hose of 0°, 45°, and 90° in different configurations. Tests were performed at different flow rates and pressures for each hose configuration. The pressures were compared across configurations to a base line reading from a hydraulic measurement bench. After a pressure adjustment factor was applied to the hydraulic test apparatus to minimize pressure drop between the two systems. Pressure deviations (>10.56 kPa) from the base line were more significant at higher engine speeds. Flow rate differences (<167 mL min^{-1}) were determined to be negligible (<0.5%). Calculated power differences (<33 W) were less than 1% of full scale power measured. This small power loss suggested that using the hydraulic measurement apparatus on a tractor would enable

accurate measurements of hydraulic power provided to implements regardless of hydraulic hose bend angles.

Keywords. Data Acquisition, Flow rate, Hydraulic power, LabVIEW, Pressure, Tractor

3.1 INTRODUCTION

When instrumenting an agricultural tractor to obtain actual operational data from the hydraulic system, mounting locations and space requirements are the most important design aspects of the system. Tractor hydraulic systems must endure the stress of intermittent use and frequent on/off cycling and are widely used for powering implements where mechanical or electrical energy are inefficient. Manufacturers install the entire hydraulic system in a relatively small space due to the power take-off shaft (PTO), drawbar, and 3-point hitch in the same area at the rear of the tractor (Fig. 3.1).

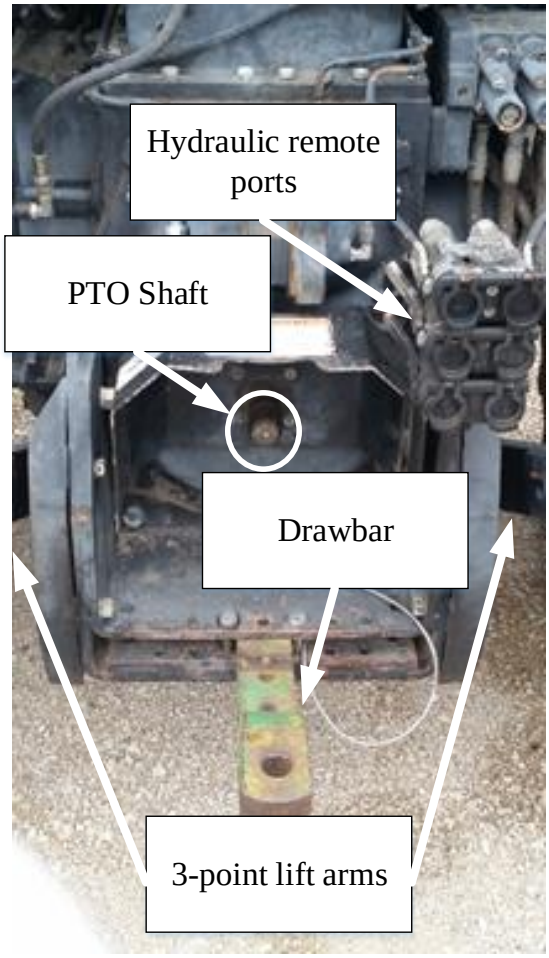

Figure 3.1. Typical locations at the rear of an agricultural tractor for delivery of power to implements.

Determining hydraulic power available for agricultural implements requires few sensors; however, implementing such systems is challenging due to space constraints (Fig. 3.1). Implement hydraulic power consumption can be determined by measuring the pressure and the flow rate of the fluid delivered to the implement. Researchers have the option of installing a flowmeter between the main hydraulic pump and the hydraulic remote ports, or as an extension between the remote ports and the connected implement. As recommended by a flow meter manufacturer, a minimum upstream conductor length of 10 times the flowmeter port diameter and a minimum downstream conductor length of

5 times the flowmeter port diameter was required (Flo-Tech, 2015). This is typically done to create laminar fluid flow in the measurement region to maximize the accuracy of flow rate readings. In a case where space is the limiting factor, having the recommended lengths of straight tubing in line with the flowmeter can be difficult. A previous study on agricultural tractor performance used a Hydrotecknik RE6 flow turbine installed in the main pump line upstream of the hydraulic remote block at the rear of the tractor (Burgun, et al., 2013). This approach limited the hydraulic implement power measurement accuracy by inducing the hydraulic system efficiencies into the measured data. The author's approach also modified a tractor part which would require that the modification be undone after the project has ceased, to ensure proper functionality after the tractor returned to normal use.

This research presents a different approach for determining the hydraulic power delivered to an implement by a tractor. The goal of this new approach was to minimize modifications to the tractor hydraulic system and allow the hydraulic power test system to mount on any tractor using standard ISO 5675 hydraulic couplers. Guidelines outlined in The Organisation for Economic Co-operation and Development (OECD) Code 2 were used for temperature and measurement tolerances. Installing a straight-line flow meter system on the rear of the tractor would not be appropriate to meet these objectives, as the hydraulic test apparatus needed to allow the 3-point lift arms and the PTO shaft to function unobstructed, without adding excessive length to implement hydraulic hoses (Fig. 3.1).

3.2 OBJECTIVES

The goal of this project was to develop a portable hydraulic pressure and flow measurement system. This system would attach to the remote hydraulic ports at the rear of the tractor with minimal modifications to determine the hydraulic power delivered to an attached implement. Specific objectives of the current research work were to:

- Determine which of the six tubing configurations used with a portable hydraulic pressure and flow measurement system could be mounted without modification to a tractor and provide adjusted pressure and flow rate measurements with differences less than 2% and 0.5%, respectively.
- Determine whether the hydraulic power obtained using the portable hydraulic pressure and flow measurement system had differences less than 1% of full scale hydraulic measurement bench power measurement.

3.3 MATERIALS AND METHODS

A complete system to test the effect of tube bend configurations on pressure and flow rate measurement accuracy was established. This system was comprised of an agricultural tractor connected with an in-line Device Under Test (DUT) and a bench hydraulic measurement test apparatuses.

3.3.1 Measuring Devices

Sensors with analog voltage signal output were selected to allow the most flexibility and compatibility with data acquisition system (DAQ) hardware, and ease of expansion into a higher order system. Following this guideline, a turbine style flowmeter (Flo-tech Activa F6206-AVB-NN, Racine Federated Inc., Racine, Wisc.) which has the

capability of measuring 15 L min^{-1} to 303 L min^{-1} with an analog output of 0 V DC to 5 V DC was selected to work with the higher flow capacities of hydraulic systems on newer agricultural tractors. The turbine flowmeter measures the bi-directional flow rate and hence only one sensor was required in the system loop. Additional benefits of the sensor design were: supplementary internal flow straighteners on both sides of the turbine and the availability of ports for installation of temperature and pressure sensors (Flo-Tech, 2015). Analog pressure sensors are widely available in a variety of pressure ranges. The selected pressure sensor (OMEGA Px309, OMEGA Engineering Inc.) was capable of measuring 0 MPa to 34.5 MPa (0 psi to 5000 psi) with a voltage output range of 0 V DC to 5 V DC (OMEGA, 2014). The data acquisition interface between the sensor assembly and the data acquisition computer was a National Instruments (NI) myDAQ (National Instruments Corporation, Austin, Texas).

The flow meter ports (25.4 mm diameter) with SAE 16 threads, were connected to a series of reducers and adapters decreasing the dimensions from SAE 16 to 19 mm National Pipe Thread (NPT), and to 19 mm (¾ in.) medium pressure hydraulic hose (NRP-Jones Hydra-Lite II, 21.4 MPa maximum pressure rating) with ISO 5675 quick-couplers. The sensors and hoses were mounted to a plywood board using U-bolts as illustrated in figures 3.2a and 3.2b. The hose ends were able to be mounted with the hose in a straight-line configuration (0°), 45°, 90°, or any combination of these bends (Fig. 3.2a, 3.2b) using the plywood board and U-bolts; however, not all combinations were used for testing. The six tubing configurations selected were: 0-0, 45-0, 45-45, 90-0, 90-45, and 90-90. The reciprocal tubing configurations: 0-45, 0-90, 45-90 were assumed unnecessary due to symmetry. When organizing the tubing configurations as the main

treatments, an orientation was selected in which the inlet and outlet were parallel but have opposite direction. For example, the male inlet coupler of the DUT would insert into the rear-facing tractor remote port and the female outlet coupler of the DUT would have the same rear-facing direction as the tractor remote port. This orientation would allow the DUT to function as an extension hose installed on a tractor (Fig. 3.2a, 3.2b).

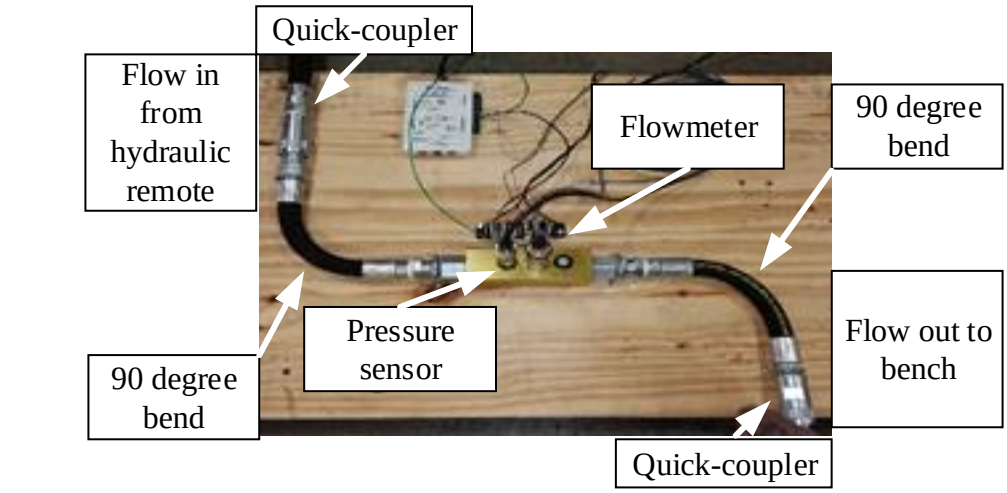

(a)

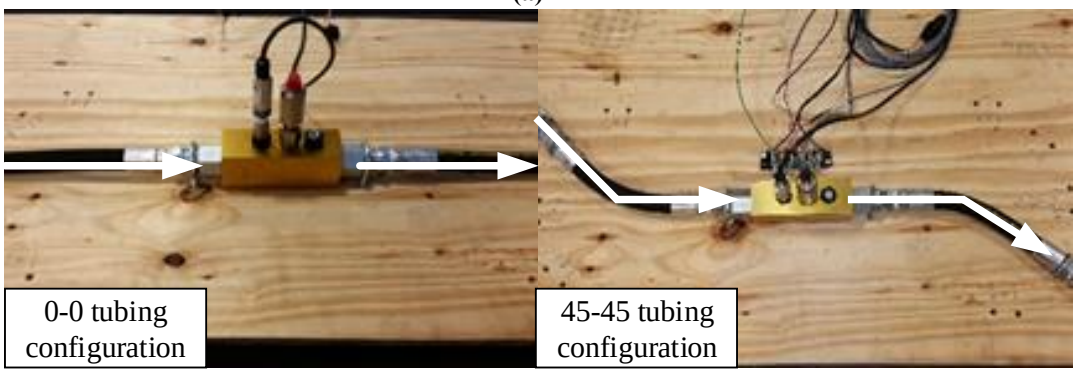

(b)

Figure 3.2 (a) DUT in a 90-90 tubing configuration, (b) DUT in 0-0 and 45-45 tubing configurations.

3.3.2 Test Setup

To test if there was an effect of the degree of bending on the accuracy of pressure or flow rate measurements, the flow rate and pressure readings from the DUT were compared to the flow rate and pressure readings from a hydraulic test bench measurement

apparatus, hereafter referred to as the Bench (Fig. 3.3).

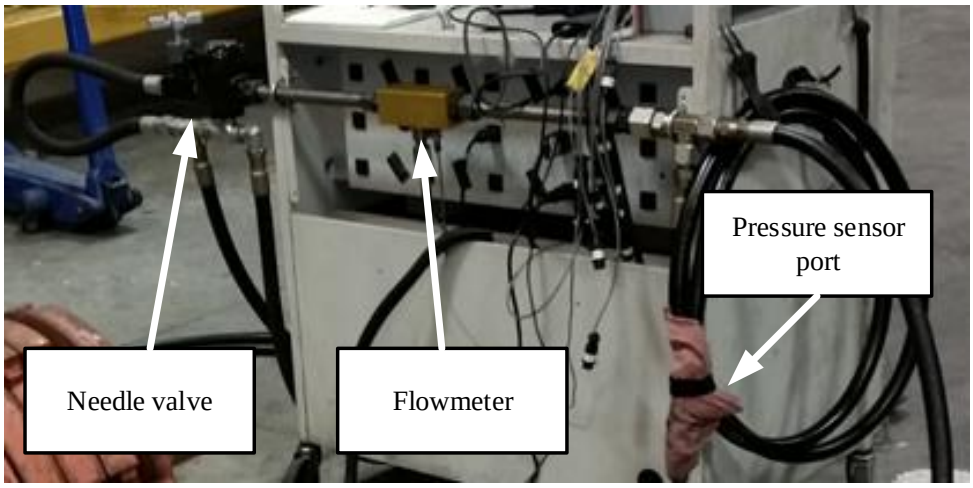

Figure 3.3. Bench test apparatus used by Nebraska Tractor Test Laboratory (NTTL).

The Bench used by the Nebraska Tractor Test Laboratory (NTTL) consisted of a Flo-tech flowmeter with the same specifications as the one used on the DUT, strain-type pressure transducers, and a needle valve. The sensors are calibrated annually, traceable to ISO 9001. The flowmeter assembly was mounted with a straight steel tubing of 30 cm (12 in.) in length and 19 mm (¾ in.) diameter, connected to hydraulic hoses of the same diameter on both the upstream and downstream sides. A DAQ board (NI cDAQ 9174, National Instruments Corporation, Austin, Texas) with analog, strain, and thermocouple modules was used for collecting the data. Further details are provided under data acquisition hardware and software program.

The DUT used the fixed position flowmeter with several coupler location options to obtain the different tubing configurations as described earlier. The systems were connected so that the DUT was connected to the tractor's extend remote port via a 19 mm (¾ in.) diameter hydraulic hose with a length of 1.8 m. Flow exiting the DUT went through the Bench system and returned to the tractor's retract remote port. This setup

placed the DUT and the Bench flowmeters and pressure transducers in series before the needle valve. A schematic illustrated in figure 3.4, depicts the connections and sensor locations of the DUT and the bench measurement apparatus in relation to the tractor providing the hydraulic flow.

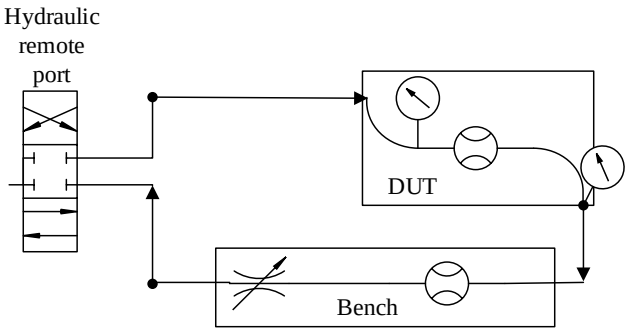

Figure 3.4. Schematic diagram showing system flow direction and sensor locations.

A Case IH tractor (DX55, CNH America LLC, Racine, Wisc.) with an engine rating of 35.8 kW at a rated engine speed of 2700 rev min^{-1} was used to generate fluid flow for the tests ranging from approximately 20 L min^{-1} to 44 L min^{-1} measured by the Bench flow meter, corresponding to different engine speeds (Fig. 3.5).

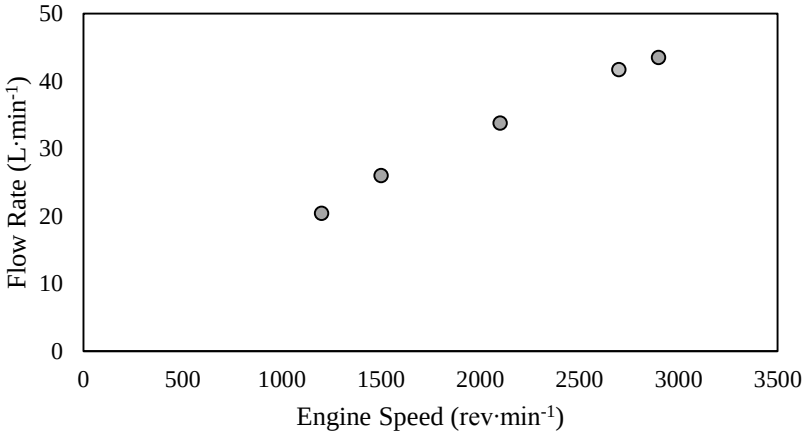

Figure 3.5. Hydraulic flow rate from one hydraulic remote versus engine speed with the tractor's hydraulic remotes adjusted for full flow.

3.3.3 Data acquisition Hardware and Software Program

A LabVIEW application programming interface (API) was created to read and log the signal data from the DUT. A graphical user interface that allowed the user to specify the channel of the pressure and flow sensors via the DUT Channels array (Fig. 3.6).

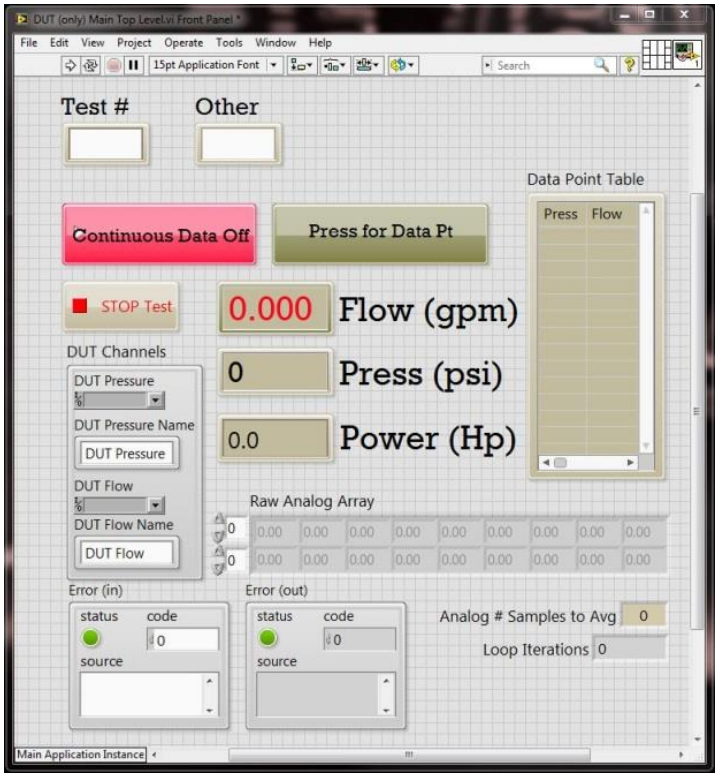

Figure 3.6. LabVIEW Front Panel for DUT testing.

Scaled engineering values allowed the flow rate, pressure, and power to be displayed in real-time to the user. “Continuous Data” push button control allowed the user to start and stop collection of mean 1 Hz raw data gathered while the control was in the “On” state, and omit data when the control was “Off”. This push button control allowed the program to run continuously, without continuous data collection. The other push button control allowed the user to collect a single 1 second mean data sample, which was helpful collecting the necessary OECD Code 2 required hydraulic performance parameters. The raw analog data were presented in an array of values at the sampling frequency of 1000

Hz.

A schematic drawing is presented in a block diagram (Appendix A) to depict the flow of data. LabVIEW has pre-generated DAQ virtual instruments (VIs) which simplified development of the block diagram program. The main components of any LabVIEW VI were initializing, reading/writing values, and closing. In order to save the data that was read, the data needed to be logged to a file.

NI myDAQ is a portable DAQ with multiple analog and digital inputs and outputs. The analog channels can be configured as either differential voltage or single ended input. A single 16-bit analog-to-digital converter was used to sample both analog channels with voltages up to ±10 V DC and sampling rates of 200,000 Hz per channel. Both analog channels were utilized as differential voltages, one channel for the pressure sensor and the other for the flowmeter on the DUT.

The API used to gather the Bench stand's results was developed for the official testing by the NTTL engineers. In the NTTL version, up to four pressure sensors could be used along with a flowmeter, fiber-optic engine speed sensor, and a thermocouple. The channels were set up in NI Measurement and Automation Explorer (NI MAX) as tasks that could be called by the API.

NI modules for data collection on the Bench included a 4-channel universal sink/source digital module (NI 9435, National Instruments Corporation, Austin, Texas) to read the digital signal of the engine speed sensor, a 4-channel thermocouple module (NI 9211, National Instruments Corporation, Austin, Texas) for ambient and hydraulic temperatures, a 4-channel bridge analog module (NI 9237 D-SUB, National Instruments Corporation, Austin, Texas) to read strain-based pressure sensors, and a universal analog

module (NI 9219, National Instruments Corporation, Austin, Texas) which measured the analog voltage output of the flowmeter. For the current tests only two strain channels for pressure sensors, the two temperature channels, and an analog voltage channel for the flowmeter were utilized.

3.3.4 Test procedure

OECD Code 2 (OECD, 2016) test requirements for tractor hydraulic power only stipulate flow and pressure to be recorded at maximum engine speed. However, operators utilize hydraulic power at various engine speeds, from low idle to maximum speed, necessitating the determination of hydraulic power usage over a range of engine speeds. The tractor used in the study had a rated engine speed of 2700 rev min^{-1}, and high idle speed of 2900 rev min^{-1}, so both speeds were chosen for the high flow rate tests. Engine speeds for lower flow rates included 1200, 1500, and 2100 rev min^{-1}, which covers the range of typical operating speeds for larger tractors with rated engine speeds of 2100 or 2200 rev min^{-1}. Using the Nebraska Tractor Test Report 1837 (NTTL, 2004) for the Case IH DX55 a pressure of 17.58 MPa (2550 psi) was listed as the maximum sustained by the pump; therefore, Bench pressure settings at minimum pressure, 3.45, 6.90, 10.34, 13.79, and 17.58 MPa (500, 1000, 1,500, 2,000, and 2,550 psi) were used during tests.

The DUT pressure was assumed to be higher than the Bench pressure at the 0-0 tubing configuration due to a pressure drop due to the friction losses in the hose and adapters, and the orifices of the quick-couplers. After determining the pressure drop across the coupler orifice would be near 227 kPa (33 psi) at the maximum flow rate, adjustment terms were developed for the DUT pressure measurements to minimize the differences in the system measurements. The adjustment terms calculated (Eq. 3.1) were

the difference between the DUT pressure and the Bench pressure at 0-0 tubing configuration for each engine speed and pressure setting:

$$P'_{DUT_{e,p}} = P_{DUT_{e,p}} - P_{B_{e,p}} \quad (3.1)$$

Where:

P'_{DUT} = Mean DUT pressure adjustment term (kPa) at the 0-0 tubing configuration

P_{DUT} = Mean DUT Pressure (kPa) from 0-0 tubing configuration

P_B = Mean Bench Pressure (kPa) from 0-0 tubing configuration

e = engine speed setting

p = pressure setting

The adjusted DUT pressure (Eq. 3.2) was the pressure after applying the adjustment terms (Eq. 3.1) for each engine speed/pressure setting.

$$P''_{DUT_{n,e,p}} = P_{DUT_{n,e,p}} - P'_{DUT_{e,p}} \quad (3.2)$$

Where:

P''_{DUT} = Mean adjusted DUT Pressure (kPa)

P_{DUT} = Mean DUT Pressure (kPa)

P'_{DUT} = Mean DUT pressure adjustment term (kPa) from 0-0 tubing configuration

n = n^{th} tubing configuration

e = engine speed setting

p = pressure setting

Starting with the DUT in a 0-0 tubing configuration, the hydraulic oil temperature

was brought up to 60°C according to OECD test procedure for hydraulic power performance steady-state laboratory test settings at a temperature range of 65°C ± 5°C (OECD, 2014). The engine speed was then set to 1200 rev min^{-1} with the needle valve fully open. Thirty seconds of the 1000 Hz data averaged over 1 second periods were collected, and then the needle valve was adjusted until the pressure at the Bench was 3.45 MPa (500 psi). This process was repeated for the subsequent pressure levels in increasing order to minimize the rate at which the oil temperature increased. A safety relief in the tractor operator's hydraulic controls, which disengaged the hydraulic lever detent, limited maximum system pressure to around 12.8 MPa to 13.2 MPa (1850 psi to 1920 psi). With this upper limit on the hydraulic system pressure, test pressure levels were reduced to: needle valve fully open, 3.45, 6.90, and 10.34 MPa. This procedure was repeated for each of the engine speeds before proceeding to the other hose configurations (45°, 90°, etc.). Three replications were made at each hose configuration (5 engine speeds x 6 tubing configurations x 4 pressures x 3 repetitions = 360 data points). The order of the tubing configuration treatments was randomized for each replicate. Within each tubing configuration, the order of the engine speed treatments was chosen randomly. The pressure level treatments within each engine speed treatment were applied in order from lowest to the highest pressures to avoid overheating the hydraulic oil. This randomization approach was used to avoid excessive delays (caused by the time required to change tubing configuration and engine speed) in completing measurements within each replicate.

Since the Bench and DUT data were logged in two independent files, for each individual test run, the two files were merged into one file with the file timestamps used

to confirm which two files to combine for each test run. The replications for each pressure/engine speed/tubing configuration were averaged together to determine each treatment mean.

Two differences were determined as results for each treatment combination: the difference between the pressure measured by the DUT and the pressure measured by the Bench, and the difference between the flow rate measured by the DUT and the flow rate measured by the Bench. ANOVA was employed to determine if there were any differences among the treatment means. The Least Significant Difference (LSD) tests were used to determine which (if any) differences among the treatment means were significant. The pressure differential was the difference between the adjusted DUT pressure and the bench test apparatus pressure. Percent difference was calculated based on the adjusted pressure difference relative to the overall Bench pressure:

$$P_{E_n} = \frac{\left(P''_{DUT_n} - P_{B_n}\right)}{P_{B_n}} * 100 \tag{3.3}$$

Where:

P_E = Pressure difference (%)

P''_{DUT} = Mean adjusted DUT Pressure (kPa)

P_B = Mean Bench Pressure (kPa)

n = n^{th} tubing configuration

3.4 RESULTS AND DISCUSSION

The mean DUT pressure was higher than the Bench pressure at the 0-0 tubing configuration as predicted. The linear regression indicates a strong correlation between

the Bench and DUT pressures (m = 1.0063), with a high coefficient of fit (R^2 = 0.9999). Pressure values outside of the measured engine speed/pressure settings were calculated using the regression equation.

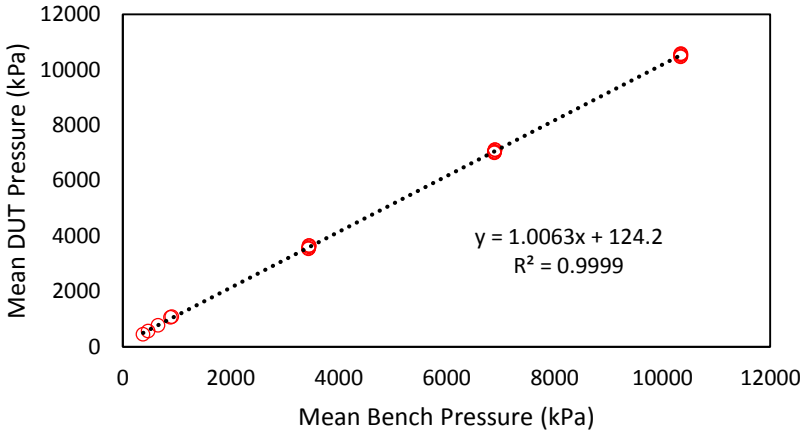

Figure 3.7. Average pressure value comparison between Bench and DUT in the 0-0 tubing configuration.

The adjustment term for each engine speed and pressure setting ranged between 72 – 242 kPa (10 – 35 psi) (Table 3.1). Pressure adjustment terms had a direct relationship with pressure and engine speed (flow rate) which was consistent with fluid mechanics theory.

Table 3.1. Adjustment terms applied to DUT pressure measurement based on 0-0 tubing configuration.

	Bench Pressure Setting (MPa)			
	Needle valve fully open	3.45	6.90	10.34
Engine Speed (rev min^{-1})	**Pressure Adjustment Term (kPa)**			
1200	72.23	93.90	112.44	127.32
1500	94.47	114.10	134.39	150.39
2100	121.89	147.97	168.61	190.50
2700	173.10	190.20	209.80	224.19
2900	171.77	197.91	221.39	241.82

Figures 3.8 through 3.10 show comparisons between the mean pressures of the Bench and the unadjusted DUT pressures for engine speeds and tubing configurations. In comparing the pressures between different tubing configurations within the 1200 rev min^{-1} engine speed, larger difference was seen at the 90-45 tubing configuration (Fig. 3.8). This higher pressure difference pattern was present in all the engine speed/pressure settings. A least significant difference value of 10.56 kPa was calculated to be statistically significant pressure differences. The 90-45 tubing configuration had statistically significantly pressure differences compared to the other tubing configurations at all engine speed and pressure setting combinations.

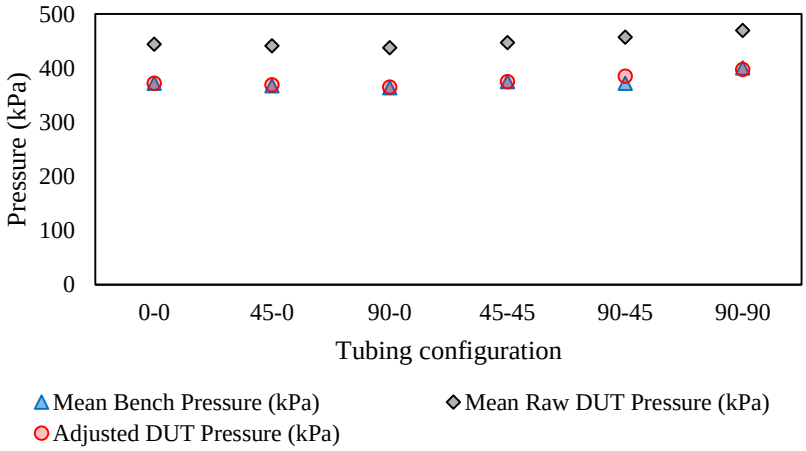

Figure 3.8. Average pressure values from test arrangements with an engine speed of 1200 rev·min^{-1} and the needle valve fully open.

Table 3.2 outlined the pressure differences and difference at low engine speed, low pressure setting. The adjusted DUT pressures (Eq. 3.2) were the pressure after applying the adjustment terms (Eq. 3.1). Pressure difference was the deviation of the adjusted DUT pressure (Eq. 3.2) from the bench pressure. The percent pressure difference (Eq. 3.3) used the adjusted pressure terms. There was no statistically significant pressure differences between treatments 1, 2, 3, 4, and 6, and treatment 5 was statistically significantly

different than all treatments. The highest pressure difference in table 3.2 of 12.9 kPa (3.47%) occurred at the 90-45 configuration when compared to other tubing configurations. OECD Code 2 allows a ±2.0 % tolerance in hydraulic system pressure (section 3.4.2, OECD Code 2, 2016).

Table 3.2. Pressure results with the tubing configurations at 1200 engine rev·min^{-1}, and the needle valve fully open (*Capital letters in superscript indicate significant differences in pressure among tubing configurations).

Treatment	DUT Tubing Configuration	Mean Bench Pressure (kPa)	Mean DUT Pressure (kPa)	Adjusted DUT Pressure (kPa)	Pressure Difference (kPa)*	% Pressure Difference
1	0-0	372	444	372	0.0^{A}	0.00%
2	45-0	367	442	369	2.1^{A}	0.57%
3	90-0	364	438	365	1.3^{A}	0.35%
4	45-45	375	448	375	0.2^{A}	0.06%
5	90-45	372	458	385	12.9^{B}	3.47%
6	90-90	401	470	398	2.8^{A}	0.70%

When comparing the pressure differences between the lowest engine speed (Fig. 3.9) and the highest engine speed (Fig. 3.10) with the “needle valve fully open”, the pressure difference increased with engine speed. As an example, at 1200 rev min^{-1} engine speed the pressure difference at 90-45 configuration was approximately 13 kPa, whereas for the same tubing configuration the pressure difference increased to approximately 28 kPa at 2900 rev min^{-1} (Fig. 3.9 and 3.10). The higher engine speeds accounted for more significant differences in the mean pressures due to a larger pressure drop across the DUT outlet/Bench inlet orifice.

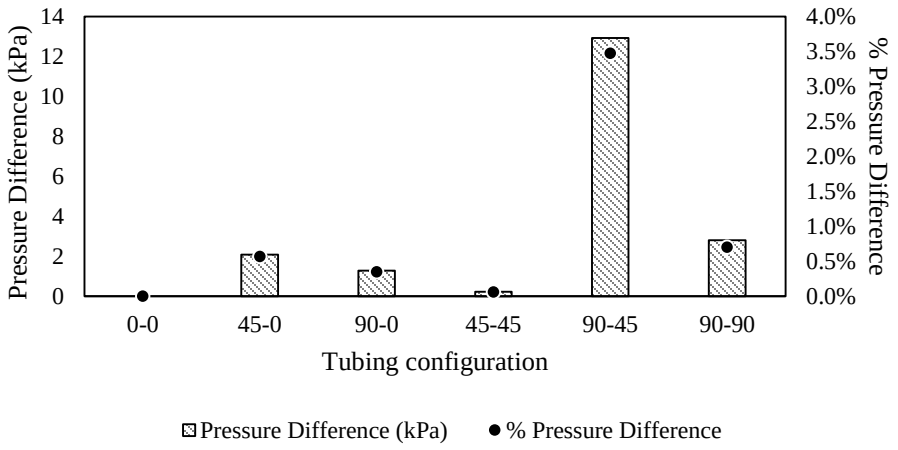

Figure 3.9. Average pressure differences of the tubing configuration with an engine speed of 1200 rev·min^{-1} and the needle valve fully open.

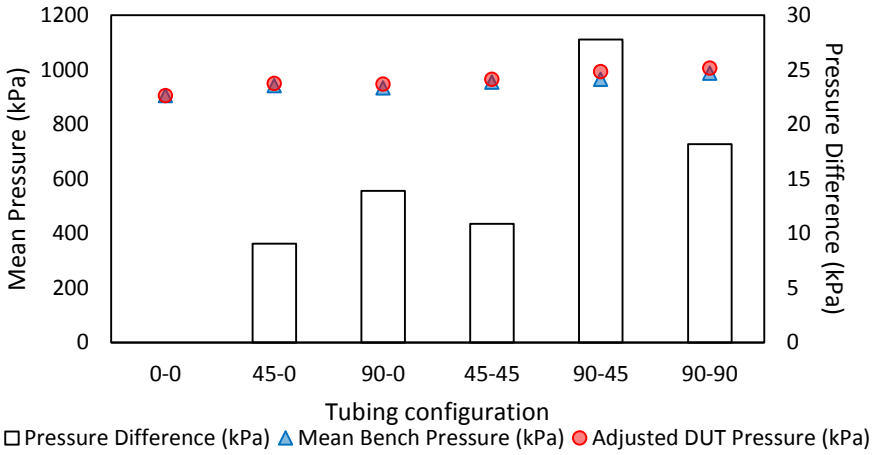

Figure 3.10. Pressure results with tubing configurations at 2900 engine rev·min^{-1} and the needle valve fully open.

A summary of pressure differentials for different DUT tubing configurations at an engine speed of 2900 rev min^{-1} is presented in table 3.3. The significant pressure differences in treatment means were between treatments 1 and treatments 3, 4, 5, and 6, and between treatment 5 and treatments 2, 3, and 4. It should be noted that the 90-45 configuration had the highest pressure difference (2.88%) of approximately 27.8 kPa.

Table 3.3. Pressure results with the tubing configurations at 2900 engine rev·min^{-1}, and the needle valve fully open (*Capital letters in superscript indicate significant differences in pressure among tubing configurations).

Treatment	DUT Tubing Configuration	Mean Bench Pressure (kPa)	Mean DUT Pressure (kPa)	Adjusted DUT Pressure (kPa)	Adjusted Pressure Difference (kPa)*	% Pressure Difference
1	0-0	905	1077	905	0.0^{A}	0.00%
2	45-0	941	1122	950	9.0^{AB}	0.96%
3	90-0	933	1119	947	13.9^{BC}	1.49%
4	45-45	954	1137	965	10.9^{BCD}	1.14%
5	90-45	965	1164	993	27.8^{E}	2.88%
6	90-90	988	1178	1006	18.2^{BCDE}	1.84%

Figure 3.11 presents the pressure differentials at the maximum operating pressure of 10.34 MPa and maximum engine speed of 2900 rev min^{-1}. When the pressure setting changed from the lowest (needle valve fully open) to the highest system pressure (10.34 MPa), there were significant differences between the mean adjusted pressures (Figs. 3.9, 3.10).

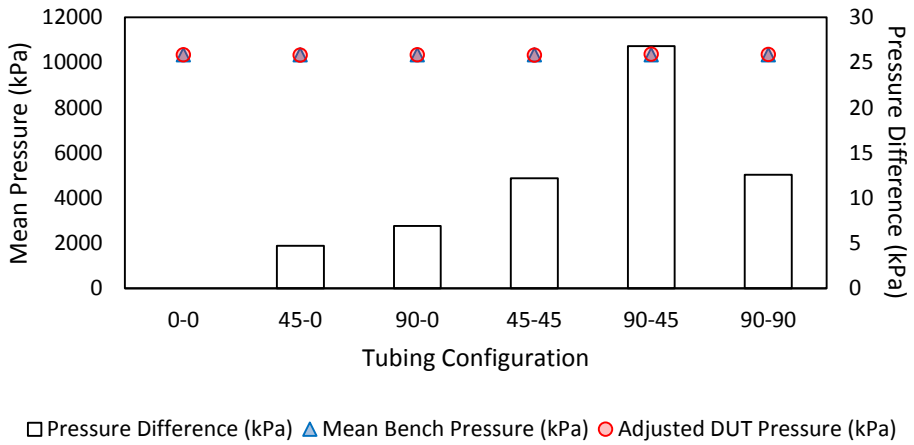

Figure 3.11. Pressure results with tubing configurations and needle valve resistance of 10.34 MPa (1500 psi) at 2900 rev·min^{-1}.

A summary of the pressure differentials for different tubing configurations at the highest system pressure (10.34 MPa) and high idle engine speed of 2900 rev min^{-1} is presented in table 3.4. It can be noted that the 90-45 configuration had the highest

pressure difference of 26.8 kPa (0.26 %) relative to other tubing configurations.

Table 3.4. Pressure results with the tubing configurations at 2900 engine rev·min^{-1}, 10.34 MPa (*Capital letters in superscript indicate significant differences in pressure among tubing configurations).

Treatment	DUT Tubing Configuration	Mean Bench Pressure (kPa)	Mean DUT Pressure (kPa)	Adjusted DUT Pressure (kPa)	Adjusted Pressure Difference (kPa)*	% Pressure Difference
1	0-0	10342	10584	10342	0.0^{A}	0.00%
2	45-0	10337	10574	10332	4.7^{AB}	0.05%
3	90-0	10336	10585	10343	6.9^{AC}	0.07%
4	45-45	10337	10566	10324	12.2^{B}	0.12%
5	90-45	10338	10606	10365	26.8^{D}	0.26%
6	90-90	10339	10594	10352	12.6^{C}	0.12%

The 90-90 configuration of the DUT is the most likely configuration for tractor hydraulic power data acquisition, given the restricted space at the rear of the tractor. This tubing configuration could also be considered as an extreme case where there is significant bending in the hydraulic hoses of the DUT. Mean bench pressures and mean adjusted DUT pressures are shown in Fig. 3.12 for each engine speed at the 10.34 MPa pressure with the 90-90 tubing configuration. Based on figure 3.11, it was observed that as the engine speed (and the flow rate) increased the pressure difference was relatively small. This trend was consistent at other operating pressures.

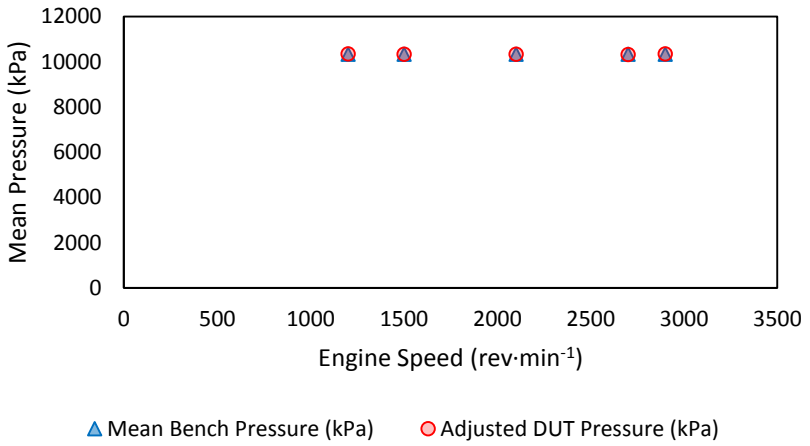

Figure 3.12. Pressure results by engine speed with the 90-90 tubing configuration and needle valve resistance of 10.34 MPa.

A summary of the pressure differentials at the 90-90 tubing configuration for different engine speeds is presented in table 3.5. A maximum difference of 13.9 kPa (0.14%) was observed at an engine speed of 2700 rev min^{-1}. Less than 0.15% pressure difference was observed at all engine speeds for the 90-90 configuration indicating that this tubing configuration can be used for hydraulic pressure data collection.

Table 3.5. Pressure results by engine speed with 90-90 tubing configuration and needle valve resistance of 10.34 MPa.

Engine Speed	Mean Bench Pressure (kPa)	Mean DUT Pressure (kPa)	Adjusted DUT Pressure (kPa)	Pressure Difference (kPa)	% Pressure Difference
1200	10338	10471	10343	5.5	0.05%
1500	10340	10498	10333	7.5	0.07%
2100	10335	10529	10332	3.7	0.04%
2700	10328	10566	10314	13.9	0.14%
2900	10339	10594	10352	12.6	0.12%

Figure 3.13a illustrates the pressure differentials with all combinations of tubing configurations and engine speeds when the needle valve was fully open. As discussed previously, the 90-45 tubing configuration consistently had the largest significant differences in pressure. The pressure differences ranged from 0 kPa at 2700 rev min^{-1} in

the 45-45 tubing configuration to 27.8 kPa (2.88 %) at 2900 rev min^{-1} in the 90-45 tubing configuration. At the system pressure of 10.34 MPa (Fig. 3.13b), the pressure differences ranged from 2.4 kPa (0.02 %) at 1200 rev min^{-1} in the 90-0 tubing configuration, to 30.4 kPa (0.29 %) at 2700 rev min^{-1} in the 90-45 tubing configuration.

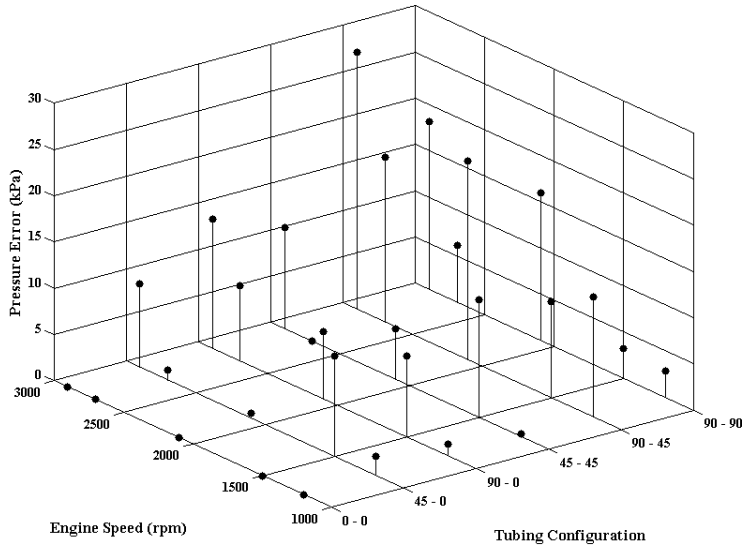

(a)

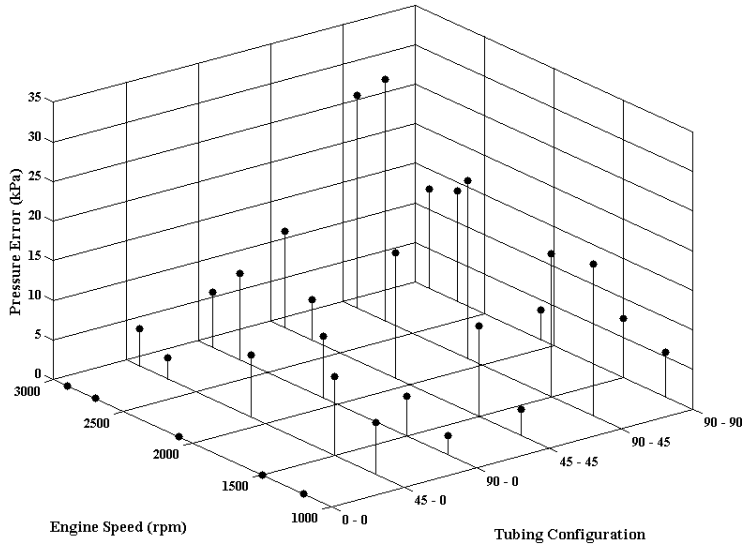

(b)

Figure 3.13. Adjusted pressure differences (%) for engine speed by tubing configuration combinations at pressure levels of (a) needle valve fully open, and (b) 10.34 MPa.

The observed mean DUT flow was lower than the Bench flow at the 0-0 tubing configuration (m = 0.9866) indicating that an adjustment term was needed for the DUT flow measurement (Fig. 3.14). The approach was the same as for the pressure adjustment (Eq. 3.1). Flow rates outside of the measured engine/pressure settings were calculated using the regression equation.

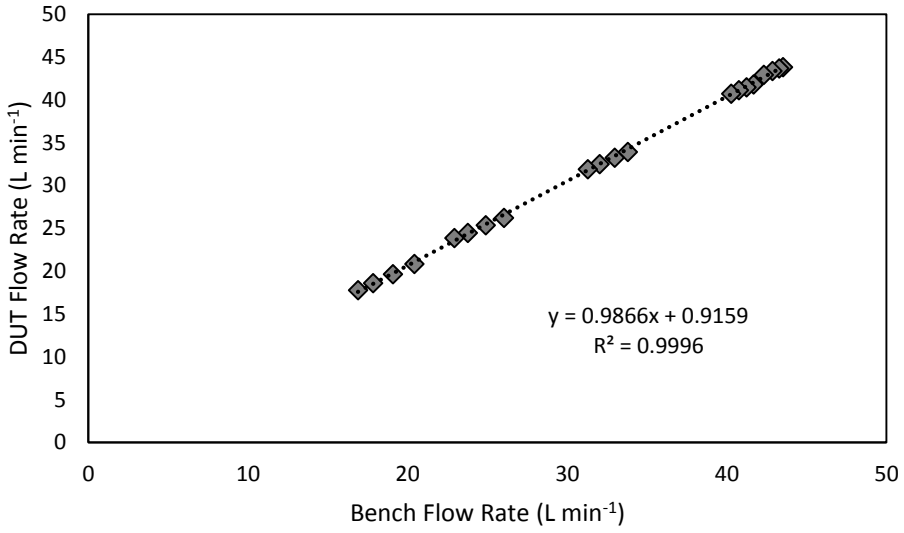

Figure 3.14. Mean Bench vs. mean DUT flow at the 0-0 tubing configuration.

The flow adjustment terms applied at each of the engine speeds are presented in table 3.6. The maximum adjustment term of 0.98 L min^{-1} (4.27 %) was applied at 10.34 MPa system pressure and the engine speed of 1500 rev min^{-1}. With increase in operating pressures the magnitudes of the flow adjustment terms increased.

Table 3.6. Adjustment terms applied to DUT flow measurement based on 0-0 configuration

	Bench Pressure Setting (MPa)			
	Needle valve fully open	3.45	6.90	10.34
Engine Speed (rev min^{-1})	**Flow Adjustment (L min^{-1})**			
1200	0.42	0.59	0.77	0.91
1500	0.22	0.47	0.72	0.98
2100	0.13	0.29	0.47	0.64
2700	0.15	0.26	0.39	0.48
2900	0.32	0.39	0.52	0.64

After the adjustment was applied, an ANOVA table was developed with a LSD value of 0.067 L min^{-1} (0.018 gal min^{-1}). Configurations which had the most significant differences between the means appeared within the 2900 rev min^{-1} range, with the largest significant difference being 0.17 L min^{-1} (0.04 gal min^{-1}, 0.38 %). However, these differences were small compared to the overall flow rate (Fig. 3.15), so it was assumed that the flow was within a reasonable difference of 0.2 L min^{-1} or approximately 0.5 percent of full scale flow rate.

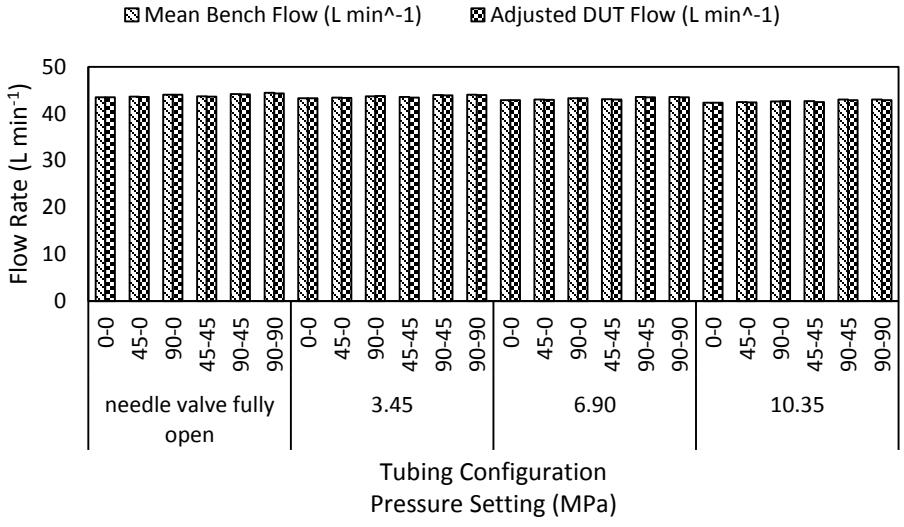

Figure 3.15. Differences in flow rate between the Bench and the adjusted DUT at 2900 rev·min^{-1}.

The power measured at the Bench and the DUT was calculated using equation 3.4, with the adjusted pressure and flow values used in the calculation for DUT power. Hydraulic power was the product of pressure and flow:

$$Power\ (kW) = \text{P (kPa)} * \frac{0.001\ m^3 * Q\ (L \cdot min^{-1})}{60\ s} \quad (3.4)$$

Where:

Power = mean hydraulic power (kW)

P = mean hydraulic pressure (kPa)

Q = mean hydraulic flow ($L \cdot min^{-1}$)

The largest differences in power occurred at the same tubing configuration/engine speed/pressure settings as the significant pressure differences. Overall, the largest difference in power occurred at the 45-45 tubing configuration at the highest engine speed setting (33 W). When considered as a percentage of the power measurement, the 45-45 tubing configuration maximum power difference was 0.46% of the Bench power.

3.5 SUMMARY AND CONCLUSIONS

A data acquisition system which was instrumented without modifying the tractor to measure and record hydraulic pressure and flow rate was successful. Using the OECD code 2 procedure for hydraulic power measurement, tests were conducted at typical engine speeds other than the governor maximum speeds. The results showed that the DUT pressure was higher than the Bench pressure as anticipated due to the pressure drop across the hydraulic fittings. Adjustments were made to correct for these system differences at the 0-0 tubing configuration. After the adjustments were made, the largest

differences occurred in the 90-45 tubing configuration with a pressure differential range of 10.4 kPa (2.24%) – 32.2 kPa (0.93%) throughout all the engine speed and pressure combinations. Higher engine speed (flow rate) settings showed larger pressure differences as expected, in the most extreme tubing configuration (90-90) with the largest difference of 21.3 kPa (0.62 %). The largest differences in the pressure measurements were at the higher engine speed settings as you would expect. These pressure differences were within OECD Code 2 permissible measurement tolerances of 2.0 %; however, the percent difference was above 2.0 % at low pressure settings due to the lower Bench pressure. Flow differences between the Bench and DUT were determined to be below 0.2 L min^{-1} (0.5 %) which was considered negligible. Significant differences in the flow rate means happened more often at the higher engine speed settings, indicating possible flow restriction through the DUT coupler. The calculated power measurement difference was also negligible (< 33 W, 0.46 %). When instrumented onto the rear of a tractor in the extreme bending case of 90-90, the differences are less than 22 W (0.44 %). With the largest power difference of 33 W, any tubing configuration could be applied. As this system will be used in field conditions and OECD Code 2 presents procedures for laboratory tests, it was determined that the differences were within the necessary measurement accuracy for field use. With these findings, it was concluded that bending in the tubing before and after the flowmeter in this system did not affect the accuracy of the power measurements.

Chapter 4 TRACTOR DRAWBAR FORCE MEASUREMENT AND VALIDATION

Abstract

Matching agricultural tractors to the implements towed by the drawbar is one of the important aspects of machinery management for ensuring optimum performance and fuel cost savings. A field deployable tractor draft force measurement and data acquisition system was developed as part of this research work. A statically calibrated drawbar instrumented to measure draft force in field operating conditions was developed. The drawbar was initially calibrated by applying loads from 4.45 kN to 134 kN using a hydraulic cylinder connected to a 444.8 kN load cell. Further testing was conducted with the drawbar installed on a tractor and tested on a concrete track using the Nebraska Tractor Test Laboratory (NTTL) load car to produce a draft loading forces. The track test consisted of seven loads corresponding to maximum power in seven gears. The draft forces as measured by the drawbar were compared to the draft measurements recorded by the load car. There were no significant differences between the means of the drawbar and load car measurements confirming that the drawbar force measurement system developed as part of this research can be used for field use. The error between draft force measurements of the instrumented drawbar and the load car measurements ranged from 0.21 kN (0.27 %) to 0.99 kN (2.88 %).

Keywords. Data Acquisition, Drawbar, Draft load, LabVIEW, Strain gages, Tractor

4.1 INTRODUCTION

The tractor drawbar is the most widely used method of towing an implement. An accurate, robust method for measuring the draft load developed by a towed implement

has been a critical industry need for some time. Tractor tests were conducted as far back as 1908 in the Winnipeg Tractor Trials (Ellis, 1913). Some approaches for draft force measurement include: attaching a load cell to the drawbar; or a hydraulic cylinder acting as a load cell, which has been used for official drawbar draft measurements at the Nebraska Tractor Test Laboratory (NTTL) as recently as 2011; installing an instrumented drawbar pin; or instrumenting the drawbar itself. An objective of this sensor was to minimize alterations to the tractor components while determining the amount of force generated by a towed implement. Fastening a load cell to the end of the drawbar was discounted as such a system created a cantilevered load that affected the tractive efforts of the tractor. In addition the load cell needed to be rigidly mounted to prevent excessive lateral movement during turning or stopping, which had the potential to cause damage to the load cell, the tractor as well as provide and unacceptable risk of personal injury to the operator. A design complication of using a load cell that would not pivot, was that the load cell proved ineffective in measuring lateral loads as seen in contour or headland operations. Another method of integrating the load cell into the drawbar was to permanently alter the drawbar which required a replacement drawbar to be installed after data collection was complete. Drawbar pin instrumentation was a possibility, but had the potential to create an unacceptable level of noise in the data due to the often large tolerances between the drawbar, pin, and implement tongue. Another approach of applying strain gages to the pin where the drawbar transfers load to the rear axle housing was suitable to reduce the noise since tolerance of this connection are well controlled. A disadvantage of this method was that since the pin rotates freely, a directional strain error was generated, minor design steps were required to ensure that the pin could not rotate

during data collection. A pin of this design requires additional development time and testing to ensure proper strain and alignment when compared to the chosen alternative.

Instrumenting the drawbar with strain gages was the most effective method for measuring draft for the intended study. One major difficulty with instrumenting the drawbar was the calibration of the strain gages on multiple agricultural machinery setups. Each drawbar needed to be calibrated, which required either an appropriate calibration test bench that could be transported to all application sites or removal of the drawbar from the test tractor for a period to allow for lab instrumentation and calibration. Previous studies have tried to determine the amount of power required to pull an implement via the drawbar including: Wendte and Rozeboom (1981), Grevis-James and Bloome (1982) and Graham et al. (1990). These studies developed data acquisition systems (DAQs) that were capable of measuring the amount of force applied to the drawbar by an implement and ground speed of the machinery with wheel slip. Graham used a hydraulic load cell attached to the end of the drawbar, while most others used a modified drawbar instrumented with strain gages. All of these studies modified a component of the tractor to measure the tractive efficiency with their main purpose being to properly size tractors for tillage and planting operations. The Organisation for Economic Co-operation and Development (OECD) requires that draft force measurements be within 1 % (section 3.4.2, OECD Code 2, 2016).

This paper presents a different approach for determining the draft force of a towed implement. This approach minimized alterations to tractor components, which allowed the system to be mounted onto multiple tractors of similar size with few modifications.

4.2 OBJECTIVES

The goal of this project was to develop a portable draft measurement system. This system would measure the draft force applied by an implement on a tractor drawbar. Specific objectives were to:

- Calibrate the instrumented drawbar , and
- Use OECD Code 2 tractor drawbar power test procedures and the Nebraska Tractor Test Laboratory load car to determine if the difference in draft measurements between the instrumented drawbar and the load car were less than 2%.

4.3 MATERIALS AND METHODS

An instrumentation system to measure and record draft force on the drawbar was developed. This system consisted of a drawbar instrumented with strain gages and data acquisition hardware. The drawbar draft force measurement system was connected to a load cell integrated into the hitch of a dynamometer car for evaluating the measurement accuracy.

4.3.1 Measuring devices

For an initial prototype design, an instrumented drawbar was deemed an appropriate device under test (DUT). The ideal location to minimize vertical loading in the strain gage measurement was as close to the front drawbar support as possible (see Fig. 4.1a). The wiring and the strain gages required protection from debris. Material was milled from the surface of the DUT to increase the sensitivity and provide a smooth surface to mount the strain gages (Fig. 4.1a). Two 90 degree strain rosettes (Micro-

Measurements EA-XX-125TQ-350, Vishay Precision Group, Inc., Wendell, N.C.) were mounted on either side of the DUT (Fig. 4.1b) to measure the axial load. A cross-drilled hole provided a raceway between the rosettes for the sensor wires to be routed safely (Fig. 4.1b). The strain gages on the rosettes were wired in a full-bridge temperature compensated configuration (Fig. 4.1c). The DUT was interfaced using a National Instruments (NI) compact DAQ (NI 9174, National Instruments, Austin, Texas) with a universal analog module (NI 9219, National Instruments, Austin, Texas) which was capable of providing the excitation voltage of +2.5 V and amplification of the strain gage signal output (Fig. 4.1d).

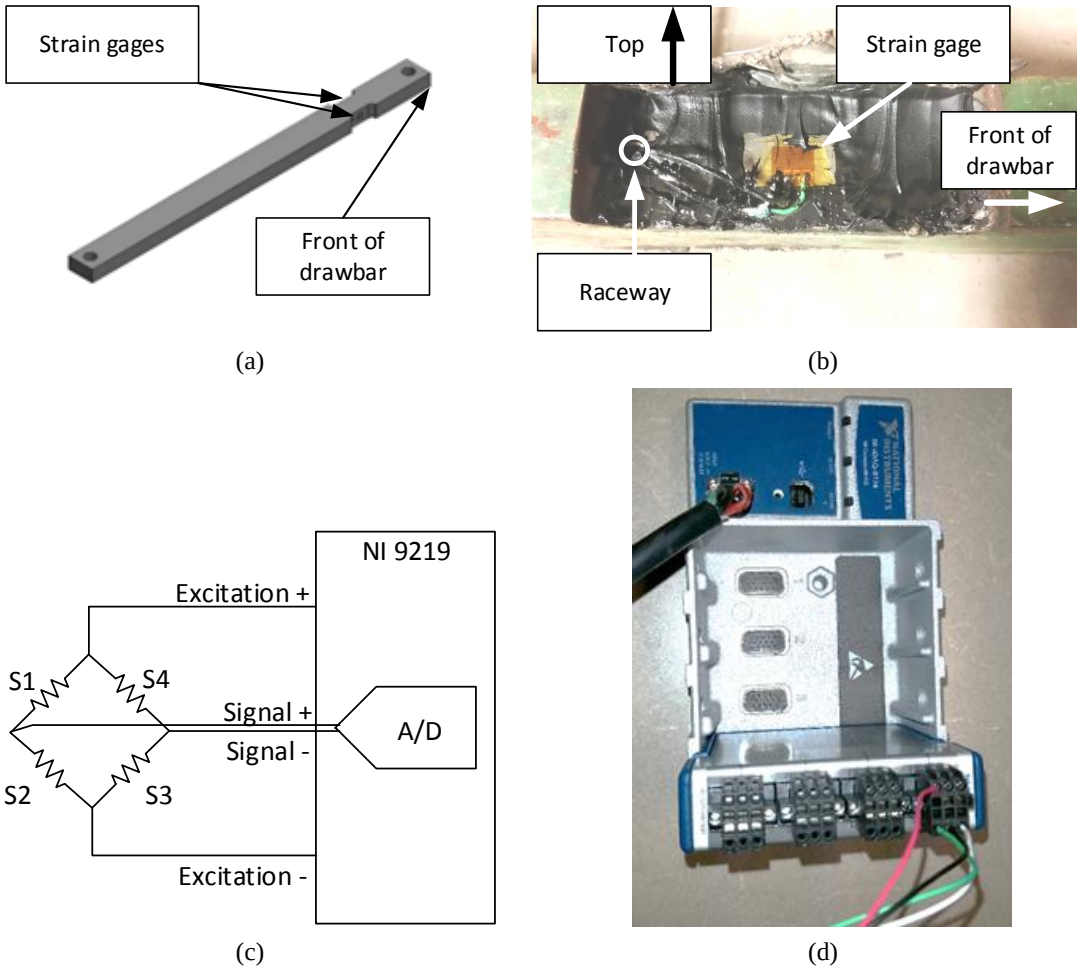

1

Figure 4.1 (a) Drawbar (DUT) illustrating sensor location, (b) focused side view where strain gage rosette was placed on drawbar, (c) Circuit diagram illustrating the bridge configuration as attached to DAQ module, (d) NI cDAQ with NI 9219 module wired as a full-bridge design.

4.3.2 Test setup

The DUT was mounted on an AGCO Allis tractor (9695, AGCO Corporation, Duluth, Ga.) in the standard centered position (tractor in Fig 4.2a). The NI DAQ board used for drawbar draft force data acquisition was connected to a laptop situated inside the tractor cab. A LabVIEW VI program was developed to record the drawbar data. The NTTL provided a calibration fixture (Fig. 4.2). The calibration fixture consisted of an Interface Gold Standard (IGS) Calibration load cell (1632AJH-100K, Interface, Inc.,

Scottsdale, Ariz.) calibrated triennial to primary standards at NIST. A hydraulic cylinder utilizing a double-acting hand pump applied a load to the load cell while the other end of the load cell was connected to the drawbar. The calibration fixture frame used a block to keep the tractor frame equidistant from the calibration fixture so that the entire system was static.

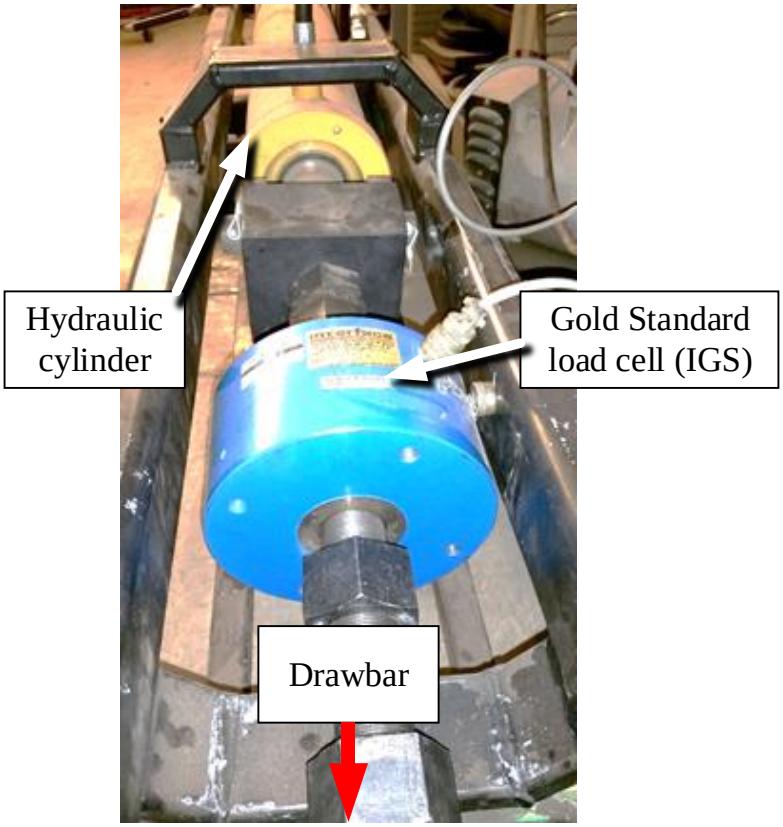

Figure 4.2. Calibration stand using a hydraulic cylinder to apply load to the drawbar

The NTTL load car (Figs. 4.3a, 4.3b) was used to apply a constant force in the plane of the drawbar with minimum vertical and transverse loading. Hitch position was set to maintain a constant distance above the ground to avoid vertical loading. The load car used two Interface load cells (1232ALD–100K-B, Interface, Inc., Scottsdale, Ariz.) connected in series and attached to the hitch to measure the draft force (Fig. 4.3c). Draft

forces are measured in the first load cell while the second load cell opposes the direction of the first to verify the load measurement. The load cells on the NTTL load car are calibrated bi-annually using the independent calibration fixture in Fig. 4.2. The drawbar test was performed on the NTTL test track, utilizing the two 244 meter (800 ft) straight lengths of concrete surface.

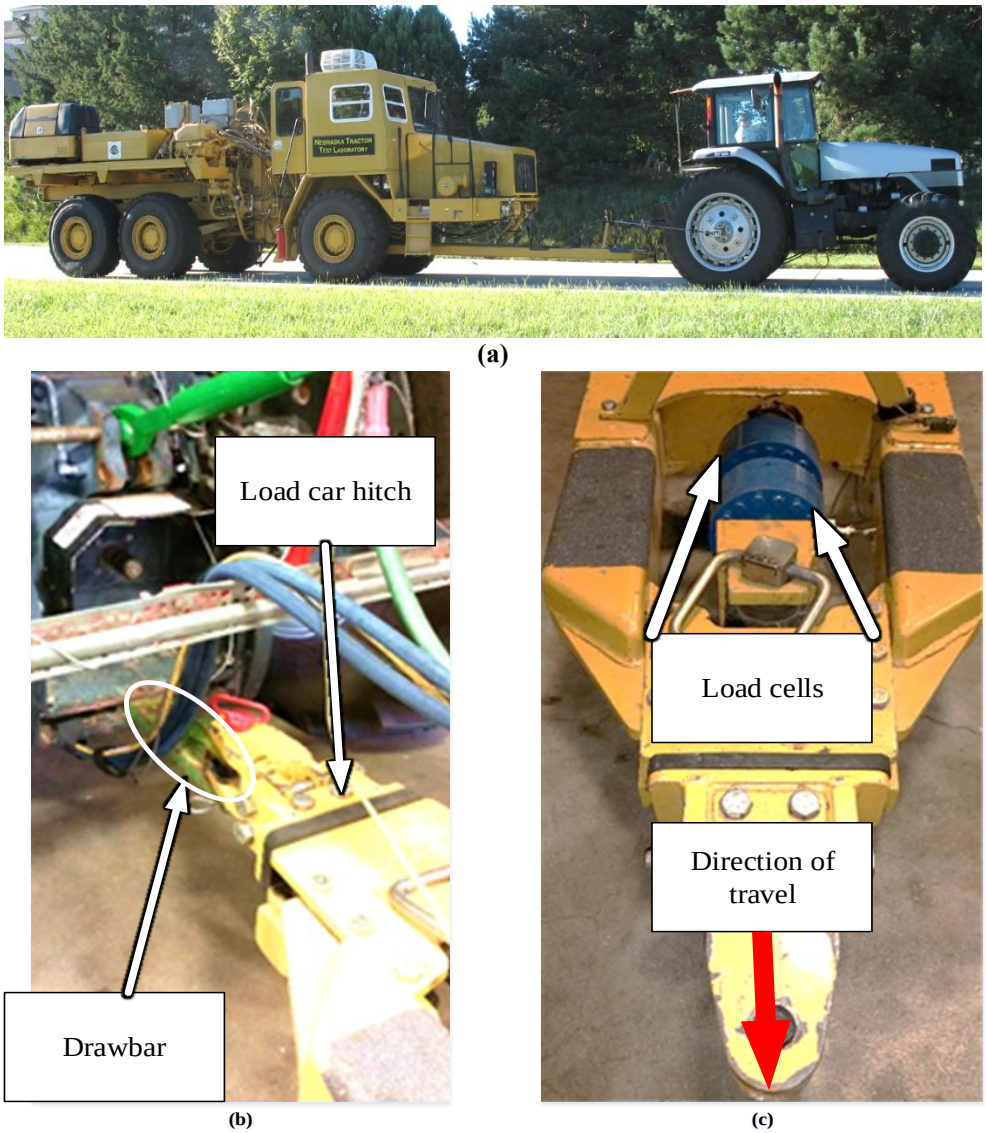

Figure 4.3. (a) AGCO Allis 9695 pulling NTTL load car for track testing, (b) detail of AGCO Allis 9695 coupled to the Test Car (c) Test Car hitch with serial load cells.

4.3.3 Calibration and Test procedure

The DUT was attached to the calibration fixture (Fig. 4.2), which uses a 444.8 kN (100 klb_f) IGS listed previously which conforms to NIST primary standards and has a static error of ± 0.017 % full scale. One side of the IGS was attached to a hydraulic cylinder which developed the tension load, whereas the other end was attached to a steel plate connected to the drawbar (Fig. 4.2). The calibration procedure began with anticipated physical loads of 4.45, 8.90, 13.3, 22.2, 44.5, 66.7, 89.0, 111, and 134 kN (1, 2, 3, 5, 10, 15, 20, 25, and 30 klb_f) as measured by the IGS. It was assumed that any load under 4.45 kN (1 klb_f) occurring during field use would be highly variable due to being either transport or a headland turn. Loads over 133 kN (30 klb_f) occurring during field use were assumed to be from heavy tillage equipment used by heavily ballasted >224 kW (>300 HP), track laying, or 4WD tractors using a higher category drawbar size. Output voltage corresponding to the strain values from the DUT were recorded during three different load cycles near the anticipated IGS physical loads and converted to match the respective IGS physical load values (Table 4.1).

Table 4.1. IGS anticipated force versus the Wheatstone bridge output for the instrumented drawbar calibration.

IGS physical force (kN)	DUT electrical value (mV/V)
2.22	0.698
4.45	0.705
8.90	0.719
13.34	0.732
22.24	0.756
44.48	0.830
66.72	0.904
88.96	0.977
111.21	1.049
133.45	1.124

Applying the calibration from table 4.1, a reiterative process was done to ensure repeatable measurements within 0.67 kN (150 lb_f).

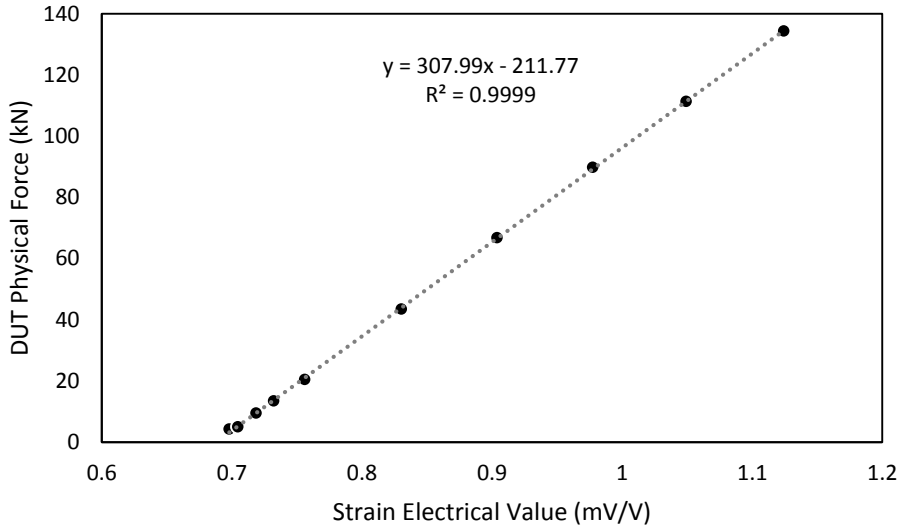

Figure 4.4. Final DUT calibration curve.

A summary of the final data values for the DUT calibration after the reiterative process are presented in table 4.2. These values were then used to create a final calibration curve equation.

Table 4.2. Final data used to determine the drawbar draft DUT calibration.

DUT physical Value (kN)	DUT Electrical Value (mV/V)
4.25	0.698
4.94	0.705
9.53	0.719
13.41	0.732
20.49	0.756
43.48	0.830
66.76	0.904
89.82	0.977
111.33	1.049
134.35	1.124

$$\text{Calibrated Force } = 307.99 * (output\ mV/V) - 211.77 \quad (4.3)$$

Where:

Calibrated Force = DUT physical force (kN)

output = Wheatstone bridge output (mV/V) of the DUT

After the determination of the calibration equation of the drawbar, testing was accomplished using section 4.4.2.1 of the OECD Code 2 (OECD, 2016). According to this section of the OECD code, the speed settings required are the gear/speed setting giving a travel speed immediately faster than the maximum power developed down to the gear/speed setting giving a travel speed immediately slower than the maximum drawbar pull developed. These operating points are further limited by Nebraska Tractor Test Board Action No. 6 (NTTL, 1998) to include only typical field operating speeds. The Nebraska Tractor Test Board requires that the maximum drawbar power shall be determined:

a. in all gears which produce less than 15% slip and a speed of less than 12.9 $km \cdot h^{-1}$ (8 mph) at rated engine speed,
b. the gear below the slowest run from part (a) with the load adjusted to produce slip near 15%, and
c. a gear producing a speed between 12.9 and 16.1 $km \cdot h^{-1}$ (8 and 10 mph) at rated engine speed.

The tractor was tested in seven gears corresponding to maximum power in each gear (gears 6 – 12) (NTTL, 1995) for typical field operating speeds. The first gear in each repetition was selected at each end of the gear range and in the middle of the gear ranges,

but due to the load car's limited transmission ranges, the subsequent gears were selected in ascending or descending order to reduce the need to adjust the load car's transmission. For example, one of the replications gear sequence was 12, 11, 10, 9, 8, 7, and then 6. Each replication consisted of four straight runs of 152.4 m (500 ft) on the concrete track in each of the seven gears. Measurements were obtained for three complete replicates of treatment combinations. Tests were carried out with the governor set to maximum engine speed. Wheel slip was measured to verify that the loading was such that none of the loads caused mean wheel slip to exceed 15 percent as required by OECD (section 4.4.1.7) (OECD, 2016) and Nebraska Tractor Test Board Action No. 6. Other data recorded by the load car were engine speed, hydraulic temperature (to verify that steady state operating conditions were achieved before beginning data collection), draft force, and ground speed. The DUT recorded the drawbar strain.

The pull from the four runs were averaged to determine the means of each treatment (gear). Differences were determined for each treatment combination: the difference between the draft force as measured by the drawbar and the draft force measured by the load car. Student's t-tests, using an alpha level of 0.025, were used to determine which (if any) of the differences in treatment means were significantly different from zero (drawbar different than Test Car measurement). As field conditions vary more than laboratory conditions, draft measurements within ±2% were considered optimal, but an accuracy of ±2.5% was considered satisfactory for farm use (Grevis-James, 1982). It should be noted that OECD requires force measurements to be ± 1.0 %.

4.3.4 DAQ Hardware and Software program

An NI 9174 cDAQ is a portable 4-slot DAQ chassis for use with NI C series I/O modules. The chassis has the capability to handle multiplexed analog I/O, thermocouples, and digital I/O signals, in the same chassis. A NI 9219 universal analog module, capable of measuring analog voltages from strain gages using bridge completion reference resistance, thermocouples, load cells, and other analog sensors, was utilized to measure the full-bridge, temperature compensated instrumented drawbar strain measurements for both calibration and testing purposes.

Separate LabVIEW virtual instrument (VI) programs were utilized for the drawbar calibration and drawbar testing. The application programming interface (API) used for calibration was the current version of the NTTL load car hitch calibration VI programmed for a NI compact reconfigurable I/O (cRIO) DAQ board. This VI was configured to measure 3 load cells simultaneously at a sampling rate of 50 Hz, so it was necessary to reconfigure the VI to measure 2 load cells (calibration fixture and drawbar). The user was required to setup channels in NI Measurement and Automation Explorer (NI MAX) to be called in the VI via a task. Push button control logic allowed some elements to be hidden on the front panel which were unused in this application. Data were logged to a file for later use to determine the calibration equation.

The graphical user interface for track testing was developed which displayed force in real-time, and setup test information (Fig. 4.5). The Get Data push button control allowed the user to log the raw data during for a specified test duration. To write the accumulated data to a file after testing was completed, the Write Data push button control was used before stopping the VI.

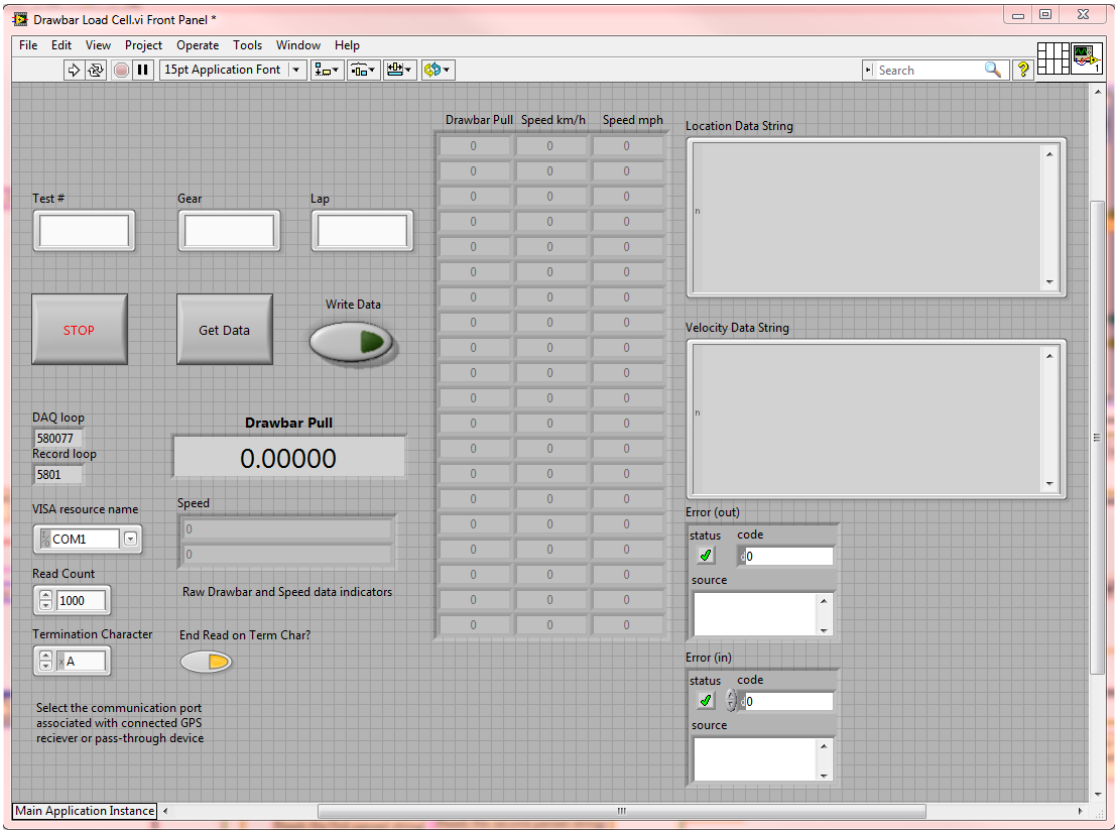

Figure 4.5. LabVIEW Front Panel for drawbar testing.

The drawbar block diagram was created utilizing similar VI controls to the NTTL hitch calibration VI (Appendix B). Tasks setup in NI MAX for calibration were used in the same capacity in the DUT VI.

4.4 RESULTS AND DISCUSSION

4.4.1 Calibration Verification

The table below (Table 4.3) shows the final calibrated DUT force values. IGS values were the result of the final DUT calibration curve replicated 3 times to verify calibration repeatability. The largest difference of the verification was at the 89 kN force with a difference of 0.53 kN (119 lbf, 0.60 %), which was within our limit of 0.67 kN.

Table 4.3. Final calibration verification.

DUT Calibration Value (kN)	IGS Force (kN)
4.25	4.16
4.94	4.75
9.53	9.48
13.41	13.42
20.49	20.48
43.48	43.61
66.76	66.48
89.82	89.29
111.33	111.34
134.35	134.57

The calibration verification (Fig. 4.6) shows that the slope of the given linear regression by the DUT was near a slope of 1.0 with relation to the force applied through the IGS. Loads below 22.24 kN (5000 lb_f) had more variability due to the smaller measurement range between treatment loads. Additional calibration below this level was unnecessary due to loading and measurement time requirements and was within procedural tolerances.

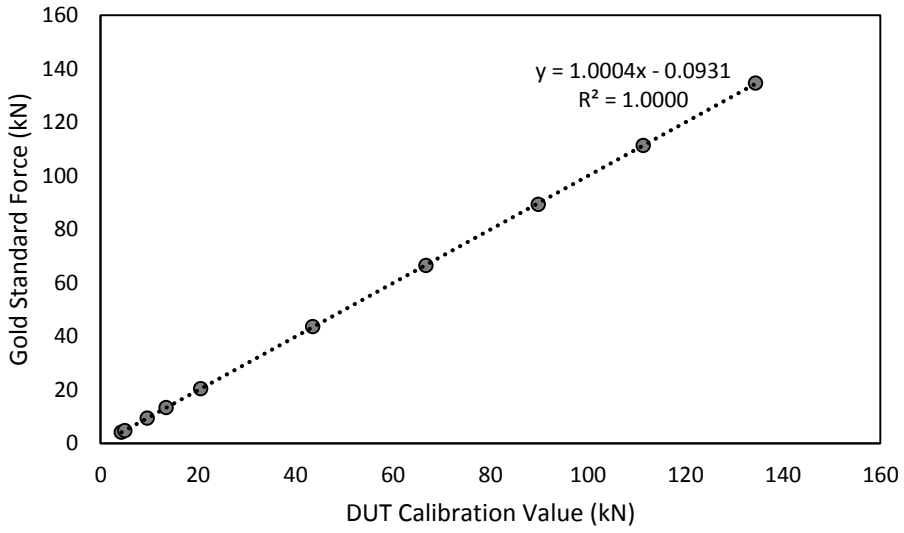

Figure 4.6. Calibration verification.

4.4.2 Track Test

The tractor equipped with the instrumented drawbar and the data acquisition system was tested on the concrete track using the NTTL load car. Data obtained during the test was averaged for each tractor gear. Student's T-tests were used to determine if there was a significant difference between the DUT and the load car draft measurements ($H_o \neq 0$ kN). A table value (t = 4.303) was obtained given a probability value of 0.05 corresponding to a 95% confidence interval and 2 degrees of freedom (3 repetitions) for a two-tailed test. Draft force differences were not statistically significantly different from zero in any of the tested gears, leading to rejection of the null hypothesis. In gear 12, the DUT measured an average of 2.55% less force as measured by the load car which was out of the 2.5% accuracy range. Gears 6 through 11 draft force averages were within 2% draft force accuracy difference (Table 4.4). Using the OECD tolerance of 1.0 % for force measurements (section 3.4.2, OECD Code 2, 2016), gears 6 through 10 met this tolerance.

Table 4.4. Average draft force results of the load car and DUT in corresponding gears.

Gear	Speed (km h^{-1})	Average load car force (kN)	Average DUT force (kN)	Average force difference (kN)	Average difference in force (%)	Average force difference standard deviation
6	4.95	81.31	81.98	-0.6713	-0.83%	0.91
7	6.10	77.00	76.79	0.2103	0.27%	0.10
8	6.88	72.82	72.30	0.5150	0.71%	0.69
9	7.84	62.71	62.17	0.5415	0.86%	0.55
10	9.17	54.42	53.98	0.4478	0.82%	0.44
11	10.89	45.71	45.01	0.7044	1.54%	0.53
12	12.80	38.67	37.68	0.9857	2.55%	0.34

Figure 4.7 shows the correlation between the force measured by the load car and the force measured by the DUT. The trend of this line (m = 1.0233) was close to the calibration curve with a strong coefficient of determination (R^2 = 0.9982) between the 2 sensors.

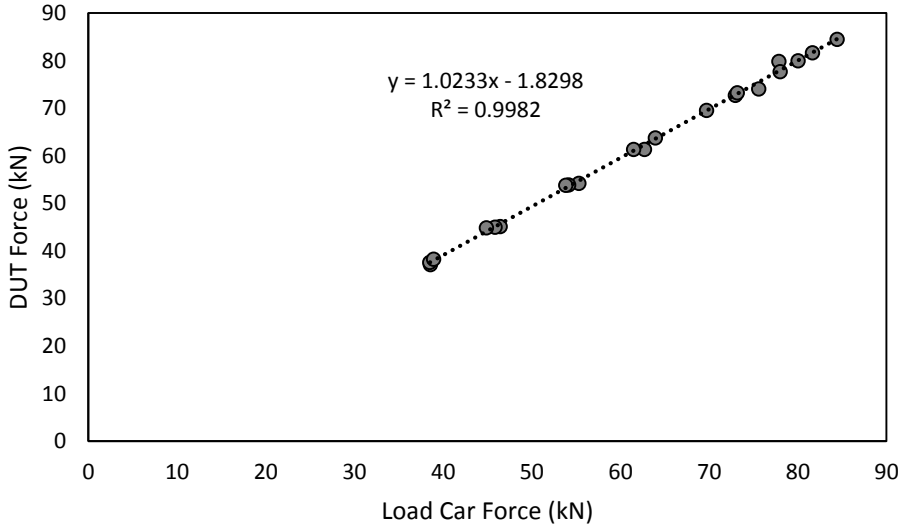

Figure 4.7. Average draft force comparison between load car and DUT for all replications of the test.

The largest average draft force difference (0.99 kN, 2.88 %) was in gear 12. The largest range of values were in gears 6 and 7 (Fig. 4.7).

4.5 SUMMARY AND CONCLUSIONS

Development of an agricultural tractor drawbar measurement and data acquisition system was accomplished. Static calibration of the DUT was successful with the DUT yielding repeatable force values within 0.67 kN (>1.5 %) of the IGS force values after the final calibration was applied. With the OECD Code 2 and Test Board Action No. 6 as the test procedures, the drawbar force was evaluated in select gears used for typical draft implement field operating speeds. Differences in draft forces between the DUT and the Test Car ($H_o \neq 0$) were not statistically significant based on the two-tailed Student's T-test using an alpha value of 0.025 leading to the rejection of the null hypothesis. With draft force differences ranging from 0.21 kN (0.27 %, gear 7) to 0.99 kN (2.55 %, gear 12) most gears provided an accuracy of less than 2.0 % error, while gear 12 was the only gear to fall outside this margin. Gears 6 through 10 were the only gears to meet the OECD force measurement tolerance of 1.0 %. However, as the OECD tolerances are possible in laboratory conditions, they are not necessary representative of plausible field measurement tolerances leading to higher acceptable tolerances of 2.5 %. These results indicate draft force measurements for field use are achievable with the drawbar draft force measurement and data acquisition system.

Chapter 5 TRACTOR POWER TAKE-OFF TORQUE MEASUREMENT AND DATA ACQUISITION SYSTEM

Abstract

Management of agricultural machinery has become an extensive research field with the mechanization of agricultural operations. Sizing tractors and implements to provide the most efficient transfer of power has become an ongoing process with advances in technology. Utilization of rotational power transferred through gear trains from the tractor engine to the power take-off (PTO) shaft has become the most efficient method of power transfer to an implement. This study used commercially available torque transducers that were installed on a tractor PTO shaft for measuring the torque delivered to an implement. Although the transducer selected was a plug and play device, the torque transducer was calibrated using the Nebraska Tractor Test Lab's (NTTL) dynamometer. The calibration followed the OECD Code 2 test procedure for varying PTO loads. After the calibration of the transducer, the calibration was verified for field conditions using the full load at varying speeds test as described in the OECD Code 2. Tractor PTO shaft torque values measured by the torque transducer were compared to the NTTL's dynamometer torque measurement. Differences in torque values measured between the transducer and the dynamometer ranged from 3 N·m to 23 N·m. Student's t-test showed no significant difference between the measurements during the full load varying speed tests which demonstrated that the sensor can be mounted on the tractor's PTO shaft for torque data collection in field operations.

Keywords. Data Acquisition, Power Take-off, LabVIEW, Tractor, Torque

5.1 INTRODUCTION

Matching implements correctly to effectively utilize tractor power has been a continuing research pursuit with the advancements in machinery technology. Annual tractor competitions in early 20th century Winnipeg were held to test: fuel and water economy, maximum engine and belt power output, draft test, and design and construction of the tractor (Ellis, 1913). The tractor transmits power to the implement through several systems independently: draft power is transferred via the drawbar or 3-point hitch, fluid power is available by way of one or more hydraulic remote blocks, rotational power is transmitted from the engine through a gear train to the power take-off (PTO) shaft, and electrical power may be provided through multiple electrical outlets inside and outside the tractor cab. The most efficient transmission (90 %) of net engine power (Fig. 1, ASAE D497.7, 2015) for an agricultural tractor to a towed implement whether stationary or mobile is via the PTO shaft (Fig. 5.1).

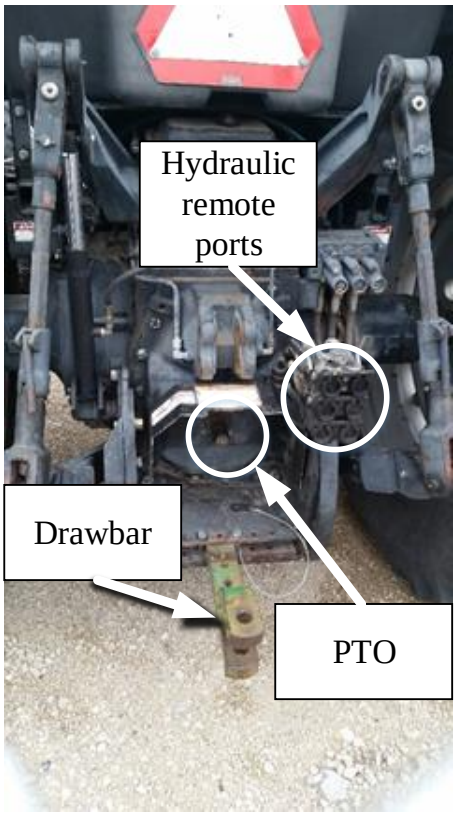

Figure 5.1. Typical location at the rear of an agricultural tractor for delivery of power to implements.

Significant changes have been made to the tractor's PTO power delivery since being commercially available for the first time in 1918 on International Harvester Company's (IHC) model 15-30 (Goering and Cedarquist, 2004). The 21-spline 1000 rev·min^{-1} shaft standard was created in 1958 followed by a 20-spline "large" 1000 rev·min^{-1} shaft. A new 1000 rev·min^{-1} shaft with 22-splines was created and included in the latest ISO standard (ISO 500-3:2014). Currently, the standard includes location and dimensions of the PTO shaft, coupler (ISO 500-3:2014), master shield, clearance zone and general safety requirements (ISO 500-1:2014). The 500-1 standard recommends the maximum PTO power that can be transmitted at rated engine speed for each PTO type. Most of the power and speed requirements of implements are calculated by the implement manufacturers and are dependent on gear boxes and implement load, while the

tractor manufacturers anticipate and calculate which tractors will be able to power these implement loads and install the appropriately sized PTO transmission.

Tractor PTO power measurement research using data acquisition systems (DAQs) have been performed utilizing fuel consumption data (Sumner, et al., 1986) to determine total implement power. Load differences between implement operations allowed the authors to estimate separation of power into draft requirements, PTO power requirements, travel requirements, and a crop load as operated for 3 minutes or one bale depending on the mode. A study by Vigneault et al. (1989) used a torque meter secured to a cart to measure PTO power. The cart was connected to the tractor drawbar and the cart could attach to an implement via the implement drawbar or the implement 3-point hitch. Limitations of such a cart were the increase in overall machinery length and a possible safety hazard if sufficiently acute steering caused the cart or implement to uncontrollably skid into the rear wheels of the tractor causing an overturn. The cart did have benefits such as the ability to connect multiple PTO types using different shafts. Bending or shear stresses on the sensor were avoided by having universal joints on both shafts connected to the sensor. Modifying the implement PTO shaft to include a built-in slip ring torque transducer was previously done for energy mapping (Kheiralla and Yahya, 2001). The modified shaft replaced the current shaft on the implement. This shaft was welded to a universal joint with a female coupler limiting the sensor to one size of PTO shaft without altering the universal joint and coupler. The rotary power table presented in the ASABE standards (Table 2, ASAE D497.7, 2015) was based on the research of Rotz and Muhtar (1992). Many of the parameters in the table are currently the same values based on the original research over 20 years ago. Not all of the rotary implements have made vast

improvements over the last two decades. However, with the increased implementation of embedded systems in agriculture, controller area network (CANBUS) and ISOBUS, variable rate application, and increasing machinery size, some parameters values may be less representative of current equipment and have become outdated. A review of the rotary power requirement data proves to become beneficial as implements emerge use the embedded systems to communicate implement power requirements with the tractor.

This paper presents a different approach to measure PTO power delivered to a towed implement. The approach used to complete this research used a commercially available slip ring torque transducer that involved no modifications to the tractor or implement PTO shaft. One of the requirements of the PTO torque sensor was the ability to fit on at least one standard PTO shaft size, allowing the sensor to be mounted onto tractors with the same size PTO shaft.

5.2 OBJECTIVES

The goal of this project was to develop a portable PTO torque and rotational speed measurement system that can attach to the tractor with no modifications to the tractor PTO shaft. Specific objectives of the research work were to:

- Calibrate the PTO sensor using OECD Code 2 tractor PTO test at varying load procedures and the Nebraska Tractor Test Laboratory dynamometer for the torque transducer, and
- Use OECD Code 2 tractor PTO full load at varying speed test procedures and the Nebraska Tractor Test Laboratory dynamometer to determine if the sensor torque and power measurements were within 1% of the dynamometer.

5.3 METHODS AND MATERIALS

A PTO data acquisition system capable of measuring and recording torque and rotational speed was developed. The system was based on instrumented slip ring transducers commercially available, to be used as the device under test (DUT). The selected transducers for torque measurement acted as an extension of the PTO shaft at the rear of the tractor. Two sensors were evaluated and one was deemed appropriate based on preliminary evaluation and testing.

5.3.1 PTO Torque Sensors

Slip-ring torque transducers with flanged ends were easily obtain commercially. However, manufacturing couplers and shafts to mount these sensors in a compact package proved to be difficult. Ready-to-use PTO torque transducers were available from two vendors (Datum Electronics, United Kingdom and NTCE AG, Germany). These sensors have PTO couplers and shafts mated directly to the measurement shaft instead of having flanged ends. The connections used for this research were the 45 mm (1 ¾ in.) 1000 rev·min^{-1} 20-spline configuration shaft and coupler.

5.3.1.1 Datum Electronics Series 420 PTO Shaft Torque and Power Monitoring System

5.3.1.1.1 Device description

The Datum PTO system (Series 420, Datum Electronics, Ltd., East Cowes, Isle of Wight, United Kingdom) was a slip-ring based torque transducer with optional shafts and coupler arrangements to meet the needs of PTO torque measurement. This sensor was not used due to safety concerns.

5.3.1.2 NCTE 7000 Torque Sensor for PTO-shafts

5.3.1.2.1 Device description

The NCTE torque sensor (7000 series, NCTE AG, Unterhaching, Germany) was a slip-ring based torque transducer with available flanged ends or a male and a clamp-type female PTO shafts (Fig. 5.3a, 5.3b).

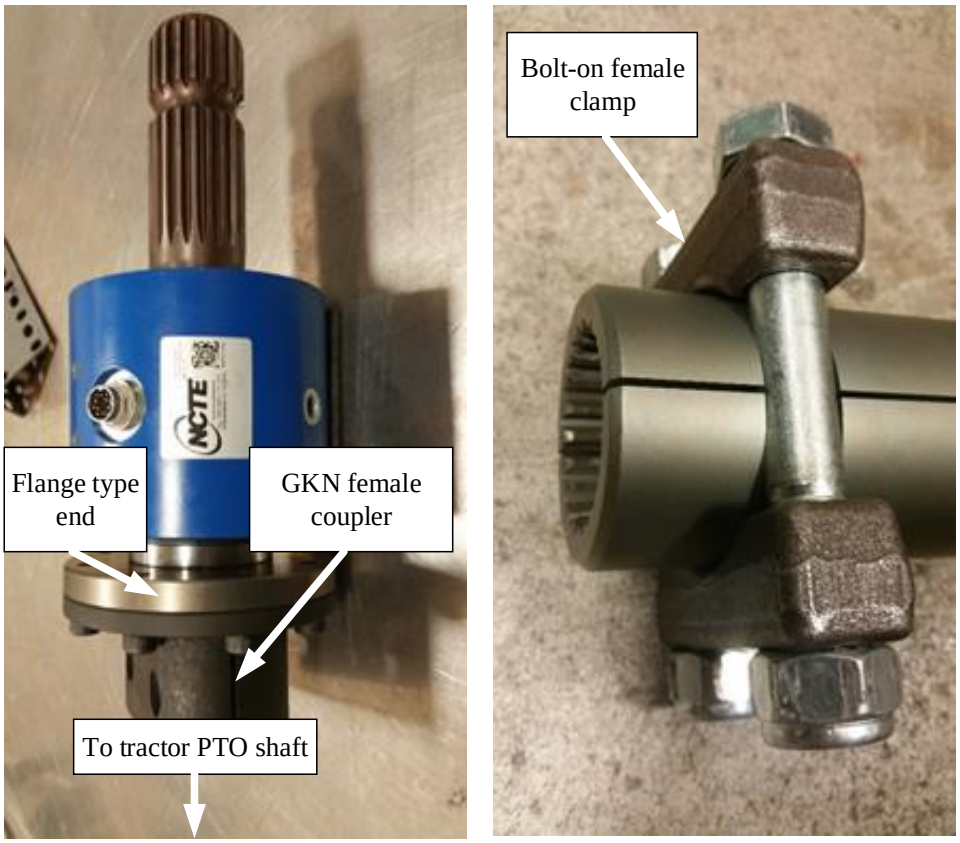

Figure 5.2. (a) NCTE torque transducer with replacement GKN female coupler, (b) Original NCTE clamp-type female PTO coupler.

Operating speeds of 3600 rev·min^{-1} and torque measurements of up to 5000 N·m were possible with this sensor. The sensor can be factory set to analog 0 - 10 V, 4 – 20 mA, or CANBUS outputs. For this study analog 0 -10 V was selected for expandable

compatibility with further instrumentation of other measurements of the implement parameters.

5.3.1.2.2 Device limitations

The clamp-type coupler (Fig. 5.3b) minimized the tolerances compared to the Datum sensor and had a run-out of <0.127 mm (0.005 in.). However, the implement PTO shaft caused the run-out to increase to ≈0.635 mm (0.025 in.). Vibration was created throughout the machine by the run-out. Similar solutions to the Datum sensor were suggested to the manufacturer and they were able to provide a simpler solution of replacing the coupler with a GKN coupler (601681, GKN Walterscheid GmbH, Lohmar, Germany). The GKN coupler had a more robust clamping method. The recessed screw, one-piece split shaft GKN coupler used bolts threaded into the coupler to provide a greater clamping force as compared to the NCTE (Fig. 5.3a).With the replacement coupler the run-out was 0.076 mm (0.003 in.) under no load and 0.381 mm (0.015 in.) connected to the implement shaft. Vibration was still present, but the relative intensity was not untypical of agricultural implement operations.

5.3.2 Calibration Equipment

The Nebraska Tractor Test Lab (NTTL) provided a 522 kW Eddy Current dynamometer (Dyno) (DM-2025DG, Dyne Systems Inc., Jackson, Wisc.) as the calibration fixture. The resistance load created by the Dyno was measured by an Interface load cell (load cell) (1110BF-2K, Interface, Inc., Scottsdale, Ariz.). The Dyno and load cell were calibrated as a system semi-annually using procedures traceable to NIST. The

load cell had two ports, one connected to the DAQ hardware for measurement purposes and the other was connected to the dynamometer controller.

5.3.3 DAQ Hardware and Software program

Data acquisition was accomplished using a National Instruments (NI) cDAQ board (NI cDAQ 9174, National Instruments Corporation, Austin, Texas). The DAQ was a portable 4-slot chassis for use with NI C series I/O modules. The chassis had the capability to handle multiplexed analog I/O, thermocouples, and digital I/O. A universal analog module (NI 9219, National Instruments Corporation, Austin, Texas) capable of measuring analog voltages from amplified bridge strain gages, thermocouples, load cells, and other analog powered sensors, was used to measure the analog output of the DUT. The digital speed signal was measured and recorded using a digital input module capable of sinking or sourcing up to 4 digital input channels (NI 9435, National Instruments Corporation, Austin, Texas). The Dyno used a digital multi-loop dynamometer (Dyno controller) (Inter-Loc V, Dyne Systems, Inc., Jackson, Wisc.) to control the torque applied or to control the speed of the PTO shaft. The Dyno data acquisition board (NI cDAQ 9188, National Instruments Corporation, Austin, Texas) was an 8-slot chassis with NI C series I/O modules to measure analog current (±20 mA) and analog input voltage (±10 V). Analog output voltage (±10 V), thermocouple signal measurements (± 78 mV), provide high speed digital I/O (5 V), digital input (250 VAC/DC), and digital output (24 V) were achievable with the Dyno DAQ. An analog input channel was used to measure the torque applied to the load cell and the high-speed digital I/O used a counter to measure the magnetic speed sensor of the Dyno. The remaining analog and digital I/O

channels were used to measure the other tractor operating parameters (e.g., intake temperature, oil pressure, engine speed, fuel flow rate).

Separate LabVIEW programs were utilized for the display and logging of the measurement data for the DUT and Dyno. The Dyno program was developed by the NTTL for official OECD tractor testing. The front panel of the virtual instrument (VI) used for the DUT during calibration was developed as part of this study (Fig. 5.4) and allowed the user to input test information to be saved as the title of the data log file (e.g., Replication 1, Torque 1). PTO speed (rev·min^{-1}) and torque (V) are displayed to the user in real-time with a table of values to be saved to the log file. The Log Data Boolean control allowed the user to log the raw 1 Hz data during specific test durations. When the Stop control was selected the data in the table was published to the data log file and the VI terminated execution.

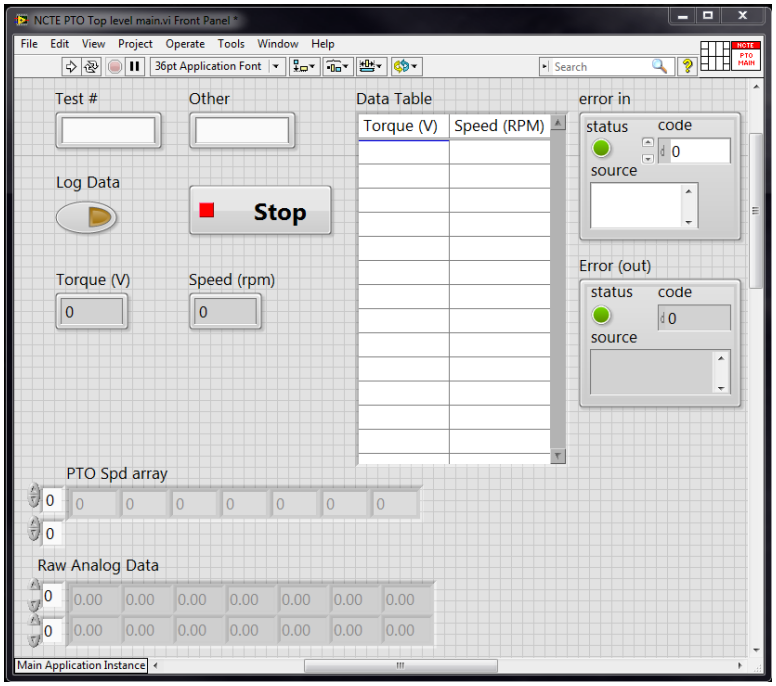

Figure 5.3. Front panel of LabVIEW program used for PTO calibration.

Torque and Speed channels for the DUT were set up in NI Measurement and Automation Explorer (NI MAX). This prevented the user from changing the physical channels during testing. In the block diagram (Appendix C), the channels from NI MAX were initialized with the log file information. A while loop allowed the program to continue to run until the Stop control was selected.

5.3.4 Test setup

Analog voltage corresponding to torque and the digital rotational speed signal of the NCTE torque sensor were read by a NI DAQ board (NI cDAQ 9174, National Instruments Corporation, Austin, Texas) installed inside the tractor cab. The laptop computer with the LabVIEW virtual instrument (VI) program used to obtain data from the DAQ board was situated away from the testing area behind a safety wall with a view of the test. The LabVIEW VI was developed to measure the DUT voltage output corresponding to torque and the rotational speed. The DUT was slid onto the shaft of the AGCO Allis tractor (9695, AGCO Corporation, Duluth, Ga.) and then the bolts were tightened to secure the DUT. A dial caliper was used to check the run-out on the implement shaft end of the DUT to ensure appropriate alignment between the mating parts. The DUT shaft end was attached to the Dyno (Figs. 5.5a, 5.5b) via a GKN PTO shaft (GKN Walterscheid, Inc., Woodridge, Ill.).

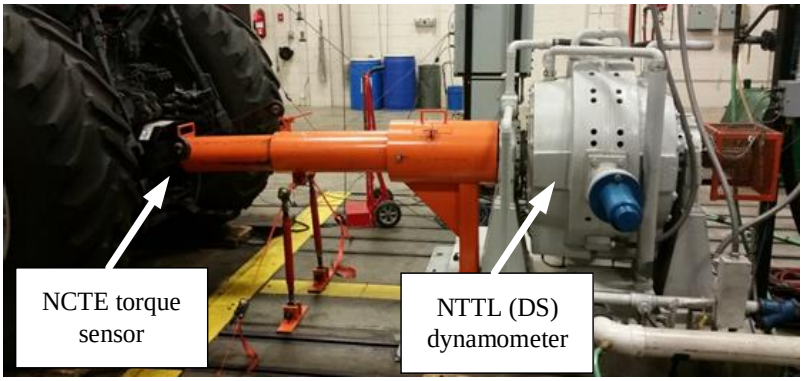

(a)

(b)

Figure 5.4. (a) AGCO Allis tractor with NCTE torque sensor connected to the DS (PTO shield extended), (b) NCTE torque sensor with PTO shield retracted.

The Dyno used an 8.90 kN (2000 lb_f) load cell (Fig. 5.6a) on a lever arm with known distance from the rotational axis of the Dyno to provide a measurable torque independently from the controller calibrated torque of the Dyno (Fig. 5.6b). The load cell has 2 output circuits to allow the Dyno controller and the measurement DAQ to have individual measurements.

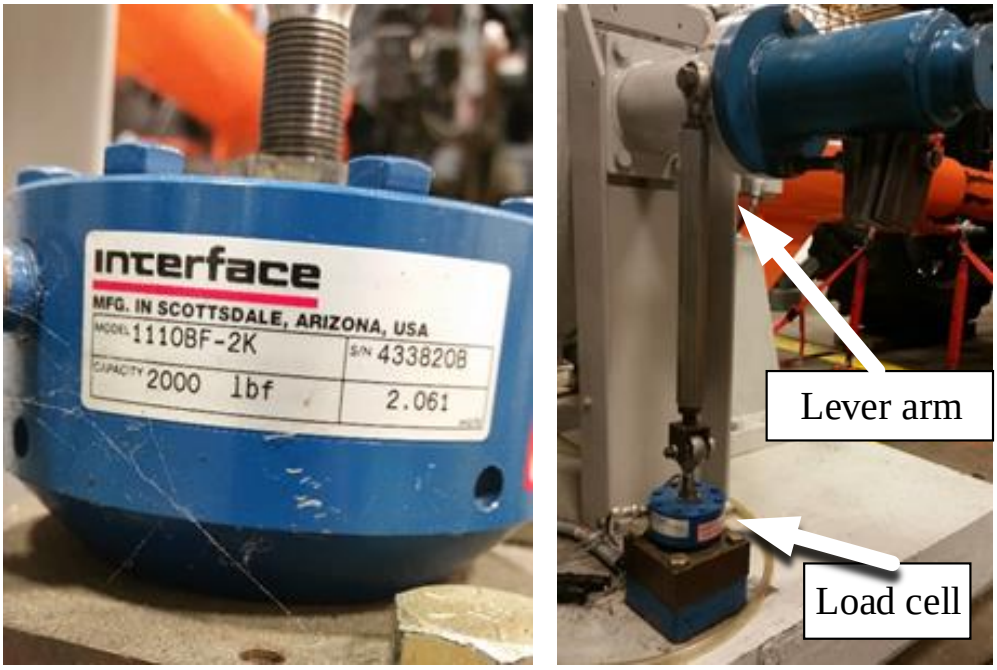

(a) **(b)**

Figure 5.5. (a) ILC mounted to Dyno base, (b) ILC with known lever arm connected to Dyno.

5.3.5 Calibration Procedure

The sensor was calibrated using NTTL's Dyno. This provided calibration conditions similar to that of a field operation, where the sensor would be operating at a fairly steady rotational speed.

Calibration began with the tractor starting the PTO at low idle (~ 600 PTO rev·min^{-1}). A load of 220 N·m was applied to limit the run-out on the unloaded shaft. The PTO speed was increased to approximately 750, 900, 1050, and 1100 rev·min^{-1} with loads 380, 570, 1070, and 1350 N·m respectively. A PTO speed of 1100 rev·min^{-1} was achieved when the tractor was at rated engine speed (RES, 2200 rev·min^{-1}), indicating a gear train ratio of 2:1.

The governor was set to wide open throttle until all the tractor power systems had become stable, a 60 second average was used for torque and speed at RES (Code 2 section 4.1.1.3.1.1, OECD, 2016). Using the Dyno controller, the torque applied through

the Dyno was set to obtain the points outlined (85%, 64%, 43%, and 21% of the torque at RES) in Code 2 sections 4.1.1.3.1.2 to 4.1.1.3.1.5 (partial loads) of OECD Code 2. The unloaded condition in section 4.4.4.3.1.6 was not used for safety concerns as the sensor shaft could potentially fail because of eccentricity in the rotation of the sensor. This process was repeated 3 times at each partial load, with 85 per cent of the torque at RES measured first in each replication. The process continued to the next lower partial load until all four points were collected in the replication. The average DUT voltage over 60 seconds at each corresponding average measured Dyno torque was utilized to create a calibration curve.

Torque at full load and varying speed (lug run) (section 4.1.1.2, OECD, 2016) was greater than the partial loads due to torque rise. The calibration equation from the partial loads was applied to the measured torque during the lug runs. Lug runs began with the engine governor set at wide open throttle. The Dyno controller applied a load to the PTO until the engine speed was reduced to RES. Additional torque was applied by the Dyno controller to reduce the engine speed in 100 rev·min^{-1} (50 PTO rev·min^{-1}) increments to minimize test duration. A 60 s average was collected for each engine speed down to 50 per cent of RES (1100 Engine rev·min^{-1}, 550 PTO rev·min^{-1}). Before the 60 second average data was taken, all signals demonstrated stability over this period. The lug run was replicated 3 times for statistical consistency of the calibration.

The difference between the 60 s averaged torque measured by the DUT and the Dyno were determined for each treatment combination. To determine which (if any) of the treatment means were significantly different from zero (DUT torque different than Dyno torque measurement) Student's t-test was used at an alpha level of 0.025.

5.4 RESULTS AND DISCUSSION

The raw voltage data from the DUT that were collected during the partial load tests were associated to torque values from the Dyno. A linear calibration regression (m = -1240.9) with a strong coefficient of determination (R^2=0.9999) was fitted (Fig. 5.7) using the four torque loads over the 3 replications.

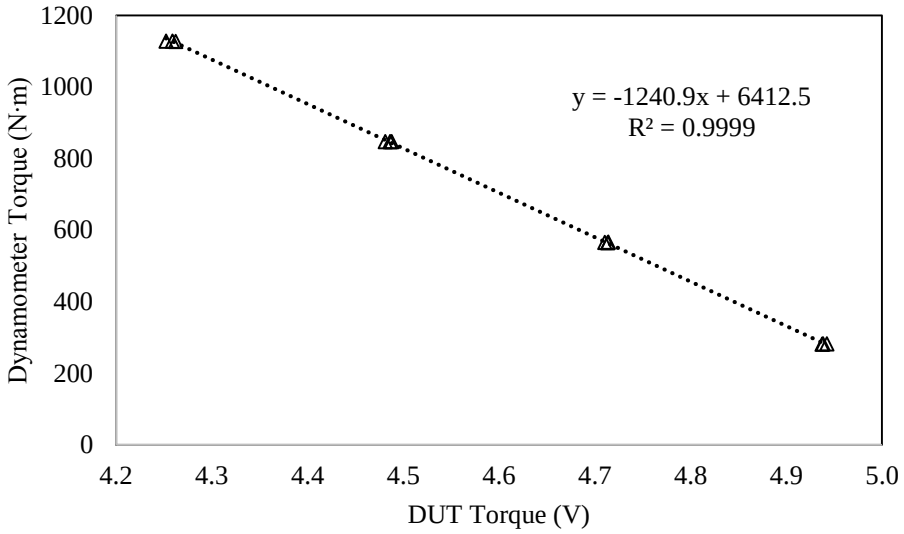

Figure 5.6. Partial loads used to determine calibration equation for the NCTE torque sensor on the tractor PTO.

The table below (Table 5.1) shows the 60 s average voltage and torque values from the DUT and Dyno respectively. Each treatment represents a load condition as outlined in OECD Code 2.

Table 5.1. Calibration points from partial loads.

Replication	% of RES Torque	DUT Torque (V)	DS Torque (N·m)
1	85 %	4.2523	1128.82
	64 %	4.4813	847.78
	43 %	4.7104	565.87
	21 %	4.9375	281.62
2	85 %	4.2589	1128.57
	64 %	4.4862	847.27
	43%	4.7136	565.01
	21 %	4.9385	282.46
3	85 %	4.2623	1127.49
	64 %	4.4879	847.69
	43 %	4.7143	566.35
	21 %	4.9425	282.23

After the calibration equation (Eq. 5.1) was formulated, the equation was then applied to the DUT voltage measured during the lug runs.

$$\tau = (-1240.9 * x) + 6412.5 \quad (5.1)$$

Where:

τ = torque measured by the Dyno (N·m)

x = voltage measured by the DUT (V)

As the tractor was lugged down with the maximum torque at the desired PTO speed, the difference in torque (≈12.5 N·m, 0.82 %) was higher in the first lug run (Fig. 5.8). The largest torque variation (≈128 N·m, 7.4 %) between the replications was at 800 PTO rev·min^{-1}, slightly below peak torque. A large drop in sustainable torque (26.5 %) was seen between 750 and 800 PTO rev·min^{-1}.

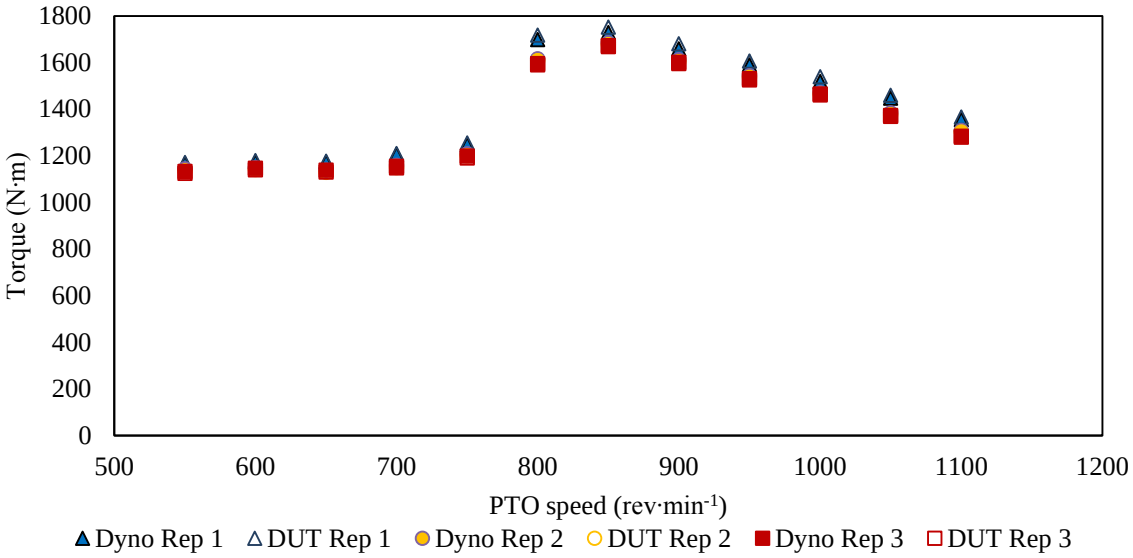

Figure 5.7. Full load varying speed tests.

Using the Student's t-tests to determine if there were any significant differences between the Dyno and the DUT torque measurements, a t-test value (t = 4.303) was obtained from the two-tailed test using α value of 0.025 and two degrees of freedom (3 replicates). No significant differences between the means of the Dyno and the DUT were observed at any of the PTO speeds. The largest differences were during the initial lug run (Table 5.2). Torque differences that ranged from 3 N·m to 23 N·m (0.27 % to 1.34 %) and were seen in the first run with the subsequent runs having smaller ranges of torque differences of 4 N·m to 9 N·m (0.29 % to 0.81 %). All torque differences were within 1.35% of the Dyno torque measurement with the last 2 repetitions within 0.81 %; OECD Code 2 required force to be ±1.0 % and the average of each treatment (PTO speed) was within ±1.0 %.

Table 5.2. Dyno vs DUT torque, full load varying speed test.

Replication	PTO Speed (rev·min^{-1})	Dyno Torque (N·m)	DUT Torque (N·m)	Torque Difference (N·m)	Torque Difference (%)
1	1100	1355.22	1365.37	-10.15	-0.75%
	1050	1446.91	1459.85	-12.94	-0.89%
	1000	1518.90	1539.30	-20.39	-1.34%
	950	1589.81	1606.26	-16.45	-1.03%
	900	1657.79	1680.09	-22.29	-1.34%
	850	1728.39	1751.36	-22.97	-1.33%
	800	1698.20	1717.87	-19.67	-1.16%
	750	1247.78	1254.42	-6.64	-0.53%
	700	1205.80	1209.02	-3.22	-0.27%
	650	1172.19	1176.94	-4.75	-0.41%
	600	1174.13	1179.68	-5.55	-0.47%
	550	1166.96	1171.27	-4.31	-0.37%
2	1100	1308.22	1301.35	6.88	0.53%
	1050	1383.84	1376.13	7.71	0.56%
	1000	1470.76	1463.54	7.22	0.49%
	950	1542.78	1535.51	7.26	0.47%
	900	1611.83	1603.79	8.05	0.50%
	850	1684.20	1676.68	7.52	0.45%
	800	1616.22	1608.06	8.16	0.50%
	750	1207.76	1199.76	8.00	0.66%
	700	1158.45	1149.18	9.27	0.80%
	650	1137.78	1128.92	8.86	0.78%
	600	1148.89	1140.48	8.41	0.73%
	550	1143.46	1134.20	9.26	0.81%
3	1100	1284.08	1279.06	5.02	0.39%
	1050	1373.31	1368.24	5.07	0.37%
	1000	1464.29	1459.99	4.29	0.29%
	950	1530.12	1524.73	5.39	0.35%
	900	1600.22	1595.19	5.03	0.31%
	850	1672.40	1667.28	5.12	0.31%
	800	1595.82	1590.23	5.60	0.35%
	750	1198.88	1190.34	8.55	0.71%
	700	1154.57	1147.19	7.38	0.64%
	650	1137.56	1129.82	7.73	0.68%
	600	1145.70	1139.11	6.59	0.58%
	550	1132.51	1124.84	7.67	0.68%

Comparing the DUT torque with the Dyno torque (Fig. 5.9), a strong coefficient of determination existed (R^2 = 0.9980). The trend of the line was linear with a slope of the differences near 1. This implied that the sensor and calibration as performed would provide consistent torque measurements in field operating conditions.

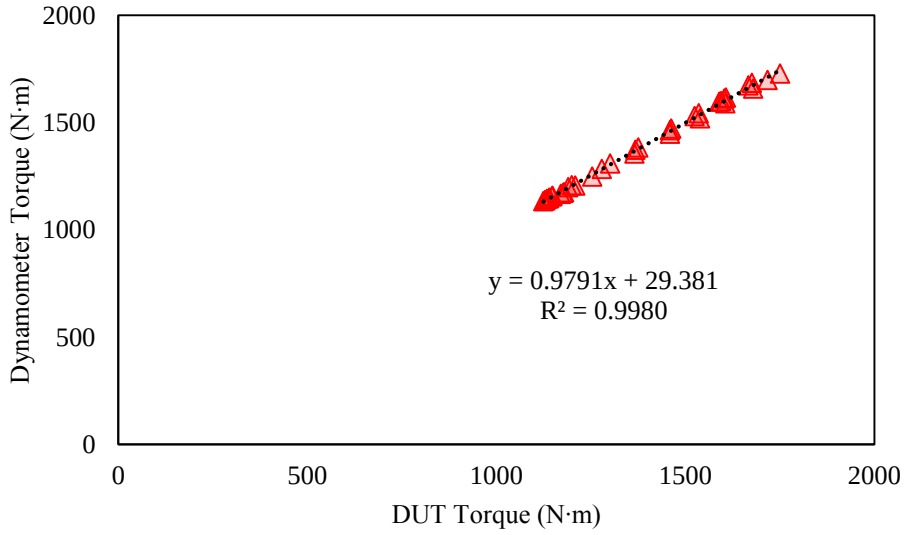

Figure 5.8. Average torque comparison between Dyno and the DUT for all replication of the lug run tests.

The power was calculated from the Dyno PTO speed and the Dyno and DUT torque measurements. PTO speed was not recorded by the DUT due to hardware or sensor limitations, which needs to be explored further. As both the Dyno and DUT output the same speed values under 650 PTO rpm, we expect a similar speed trend to continue beyond 650 PTO rpm.

Mean differences in power were less than 0.33 kW (0.38%) during the lug runs. Using a two-tailed Student's t-test at an alpha level of 0.025 for two degrees of freedom (3 replications), there were no statistically significant differences in power measurements of the Dyno or DUT.

Table 5.3. Calculated Power difference between the DUT and Dyno.

PTO Speed (rev·min^{-1})	Dyno Power (kW)	DUT Power (kW)	Power Difference (kW)
1100	152	152	0.07
1050	154	154	-0.01
1000	155	156	-0.31
950	155	155	-0.13
900	153	153	-0.29
850	151	151	-0.31
800	137	137	-0.17
750	96	95	0.26
700	86	86	0.33
650	78	78	0.27
600	73	72	0.20
550	66	66	0.24

5.5 SUMMARY AND CONCLUSIONS

A data acquisition system was implemented to measure and record torque from a tractor PTO shaft without modifying the tractor or implement shafts. The NCTE torque transducer was used for steady state calibration due to the tighter tolerances in the coupler. As a calibration procedure, OECD Code 2 was used to measure torque at partial loads to determine a calibration equation. Partial loads provided a linear (m = -1240.9) calibration equation with high coefficient of determination (R^2 = 0.999) to calculate the torque of the DUT from the amplified bridge voltage logged during the lug runs. The OECD Code 2 torque at full load and varying speed was then used to verify the calibration from measured torque at partial loads. Differences in torque between the Dyno and the DUT ($H_o \neq 0$) were not statistically significantly different from zero using a two-tailed Student's T-test at an alpha level of 0.025, leading to rejection of the null

hypothesis. Torque differences ranged from 3 N·m (0.27 %) to 23 N·m (1.33 %) during the first lug run. These differences were within 1.35% of the Dyno torque measured. Differences in the second and third lug runs had smaller torque differences within this threshold and the average treatment mean was under ±1.0 %. Power differences were within 0.33 kW (0.38 %). As the OECD Code 2 measurement tolerances for torque would be ±1.0 % in laboratory settings and the system meet the torque requirements, it was determined that the system would provide reliable tractor PTO torque measurements under field conditions.

Chapter 6 CONCLUSIONS AND FUTURE DEVELOPMENT OPPORTUNITIES

6.1 CONCLUSIONS

The portable data acquisition systems developed as part of the research presented, were successful in measuring hydraulic power, drawbar draft force, and PTO torque with minimal alterations to the tractor. The systems were developed using analog instrumentation to allow for future integration into a single system. Each system could be utilized for implement field tests to collect measurements under field conditions to determine implement load and work cycles. These tests would provide necessary data to support updates to the agricultural machinery standards (ASABE D497.7).

6.2 FUTURE DEVELOPMENT

Following this research, the next step of the project is to combine the systems into a single DAQ and collect operational profiles for fieldwork. The most important task in the future is creating a single LabVIEW program to measure and record all three energy

flows through the implement interface. An additional system parameter of value to collect is Controller Area Network (CAN) bus data (Stone et al., 2008). Engine speed, fuel consumption, and engine torque provides details on implement load cycles; such as: headland turn load, working load, contour load, and transport load (Pitla et al., 2016). Fan speed and engine temperatures characterize the engine cooling capacity and the power consumed to achieve the necessary cooling under loaded conditions. Possibilities arise with manufacturer cooperation into additional channels used to calculate hydraulic flow and hydraulic pressure, PTO torque and speed ratio, 3-point lift height, and ISOBUS implement parameters. The DAQ system would compare the reliability of CANBUS data to the instrumented sensors. Individual sensors and CANBUS measurement data would be used to create calibration equations to minimize errors in the CANBUS data. Having accurate CANBUS data, updated collection methods would be imposed to gather real-time data. This data would lead to simpler and more cost effective methods of data collection in the future by streamlining the amount of added instrumentation necessary to make these measurements. The data could then be used to create an interactive implement energy and performance database version of the ASABE D497.7 standard. The database could recommend implements to operators commonly used in the operator's region, soil types, and tractor performance range.

Several additional questions could be explored to improve results in future hydraulic research. The current tests were accomplished on a small tractor (flow ≈ 45 L min^{-1}), flow tests at higher flow rates (>200 L min^{-1}) would be beneficial to ensure the pressure differences do not become more significant with increased pressure drop from increased flow rate. Expanding the hydraulic program to allow thermocouples to be

mounted with the flowmeters would allow an indication on typical warmup times during operation and thermodynamic cooling properties.

A needed signal for draft power calculations would be velocity. Programming difficulties limited the collection of velocity measurements during testing. To overcome this issue, a more robust GPS receiver should be used, and possibly limit research measurements to only tractors with the GPS receiver connected to the Virtual Terminal of the tractor. Instrumenting the drawbar would not be the most practical way to move from one tractor to another. Designing and testing the front drawbar pin as a lightweight alternative to the instrumented drawbar is recommended. After initial calculations are made, the design would have differences dependent primarily on the tractor manufacturer and are more easily replaced on the tractor. Several manufacturers use the same diameter pin with various lengths for similar sized tractors and drawbar categories. This would also reduce the time in calibration of the pin, as a smaller cylinder fixture could be implemented. With this smaller fixture, calibrations could be performed in the field for verification.

The problems associated with the two PTO transducer female couplers evaluated for this study pointed to the need for various improvements. The coupler could be replaced with a tapered shaft design to minimize the runout experienced and reduce unwanted shaft vibration. However, using a tapered shaft will increase the coupler costs and create problems when removing the sensor from the tractor, but the benefits (e.g., installation time) could outweigh these issues. During testing of the PTO for torque measurement, it was noticed that PTO speeds above 650 PTO rev·min^{-1} were not displayed correctly. It was believed to be a hardware issue with the NI 9435 digital input

module. The NI 9401 high speed digital I/O module would be more suitable for the magnetic speed sensor in the transducer. If more transducers are purchased for future work, the flanged ends proved to be more economical since the coupler and shafts of the NCTE sensor could be swapped for different PTO configurations. The concerns of custom couplers and shafts were based on the eccentricity due to design and manufacturing potentials.

Chapter 7 REFERENCES

ASABE Standards. (2011). D497.7: Agricultural Machinery Management Data. St. Joseph, Mich.: ASABE.

Burgun, C., Lacour, S., Delacroix, A., Descombes, G., and Doyen, V. (2013). Computing time and fuel requirements to assess efficiency of a field work from conventional laboratory tests: Application to a plowing operation. Agric. Food Sci., 22(2), 247-261. http://ojs.tsv.fi/index.php/AFS/article/view/7629/6310

Ellis, L. W. (1913). Scientific American. Scientific American, 109(10), 201-204. doi:10.1038/scientificamerican09061913-201

Flo-Tech. (2015). Installation and Operating Instructions. Racine, Wisc. Racine Federated Inc. http://www.badgermeter.com/Badger-Files/PDFs/Industrial-Products/SEN-UM-00987-EN.pdf?

Goering, C., and S. Cedarquist. (2004). Why 540? Resource Magazine (Oct. 2004). St. Joseph, Mich.: ASAE.

Graham, W.D., L.D. Gaultney, R.F. Cullum. (1990). Tractor instrumentation for tillage research Appl Eng Agric, 6, pp. 24–28. http://elibrary.asabe.org/azdez.asp?AID=26339&t=2

Grevis-James, I. W. and P. D. Bloome. (1982). A tractor power monitor. Trans of the ASAE 25(3):595-597. https://elibrary.asabe.org/azdez.asp?AID=33579&T=2

ISO. 2014a. ISO 500-1: Agricultural tractors - Rear-mounted power take-off types 1, 2, 3, 4 – Part 1: General specifications, safety requirements, dimensions for master shield and clearance zone. Geneva, Switzerland: ISO.

ISO. 2014b. ISO 500-3: Agricultural tractors - Rear-mounted power take-off types 1, 2, 3, 4 – Part 3: Main PTO dimensions and spline dimensions, location of PTO. Geneva, Switzerland: ISO.

Kheirella, A.F., Yahya, A. (2001). A tractor instrumentation and data acquisition system for power and energy demand mapping. Pertanika J. Sci. Technol. 9 (2), 1-14.

Lech, M., Winter, R. DLG-PowerMix-App. Deutsche Landwirtschafts-Gesellschaft e.V. http://www.dlg.org/searchpowermix.html. Accessed 11 May 2015.

McLaughlin, N. B., C. F. Drury, W. D. Reynolds, X. M. Yang, Y. X. Li, T. W. Welacky, and G. Stewart. (2008). Energy inputs for conventional primary tillage implements in a clay loam soil. Transactions of the ASABE. 51(4):1153-1163. St. Joseph, Mich: ASABE.

NTTL. (1995). Nebraska Tractor Test Laboratory Reports. Test 1700. Lincoln, Neb.: Nebraska Tractor Test Board. http://digitalcommons.unl.edu/tractormuseumlit/2009

NTTL. (1998). Action No. 6: Maximum Drawbar Power Runs. Lincoln, Neb.: Nebraska Tractor Test Board. http://tractortestlab.unl.edu/documents/ttl_action6.pdf

NTTL. (2004). Nebraska Tractor Test Laboratory Reports. Test 1837. Lincoln, Neb.: Nebraska Tractor Test Board. http://tractortestlab.unl.edu/documents/DX55.pdf

NTTL. (2013). Nebraska Tractor Test Laboratory Reports. Test 2039:2045; 2069:2073. Lincoln, Neb.: Nebraska Tractor Test Board. http://tractortestlab.unl.edu/testreports

NTTL. (2014). Nebraska Tractor Test Laboratory Reports. Test 2093. Lincoln, Neb.: Nebraska Tractor Test Board. http://tractortestlab.unl.edu/testreports

NTTL. (2015). Nebraska Tractor Test Laboratory Reports. Test 2108:2112. Lincoln, Neb.: Nebraska Tractor Test Board. http://tractortestlab.unl.edu/testreports

NTTL. (2016). Nebraska Tractor Test Laboratory Reports. Test 2126; 2133:2135; 2150. Lincoln, Neb.: Nebraska Tractor Test Board. http://tractortestlab.unl.edu/testreports

OECD. (2016). Code 2 OECD Standard Code for the Official Testing of Agricultural and Forestry Tractor Performance. Paris, France: OECD. http://www.oecd.org/tad/code/02%20-%20Code%202%20-%20Final(February%202016).pdf. Accessed 15 March 2016.

OMEGA. (2014). Specifications Sheet. OMEGA Engineering Inc. http://www.omega.com/pressure/pdf/PX309-5V.pdf

Pitla, S.K., N. Lin, S.A. Shearer and J.D. Luck. (2014). Use of controller area network (CAN) data to determine field efficiencies of agricultural machinery. Appl. Eng. Agric., Vol. 30(6): 829-839.

Pitla, S.K., J.D. Luck, J. Werner, N. Lin and S.A. Shearer. (2016). In-field fuel use and load states of agricultural field machinery. Electronics Agric. 121:290-300.

Ricketts, C. J. and J. A. Weber. (1961). Tractor Engine Loading. Agricultural Engineering. 42(5):236- 239, 250, and 252. St. Joseph, Mich: ASABE.

Rotz, C.A. and Muhtar H.A. (1992). Rotary power requirements for harvesting and handling equipment. Applied Engineering in Agriculture, 8: 751-757

Stone, M., Benneweis, R., Van Bergeijk, J., 2008. Evolution of electronics for mobile agricultural equipment. Trans. ASABE 51 (2), 385–386–390.

Sumner, H. R., R. E. Hellwig and G. E. Monroe. 1986. Measuring implement power requirements from tractor fuel consumption. Trans. ASAE 29(l):85-89.

Vigneault, C, G. ST. Amour, D.J. Buckley, D.I. Masse, P. Savoie and D. Tremblay. (1989). A trailer-mounted PTO torque meter system. Can. Agric. Eng. 31(1):89-91.

Wendte, K.W. and H. Rozeboom. (1981). Data acquisition for tillage energy evaluation. ASAE Paper No. 81-1045, ASAE, St. Joseph, MI.

Chapter 8 APPENDICES

8.1 APPENDIX A – LABVIEW HYDRAULIC BLOCK DIAGRAM

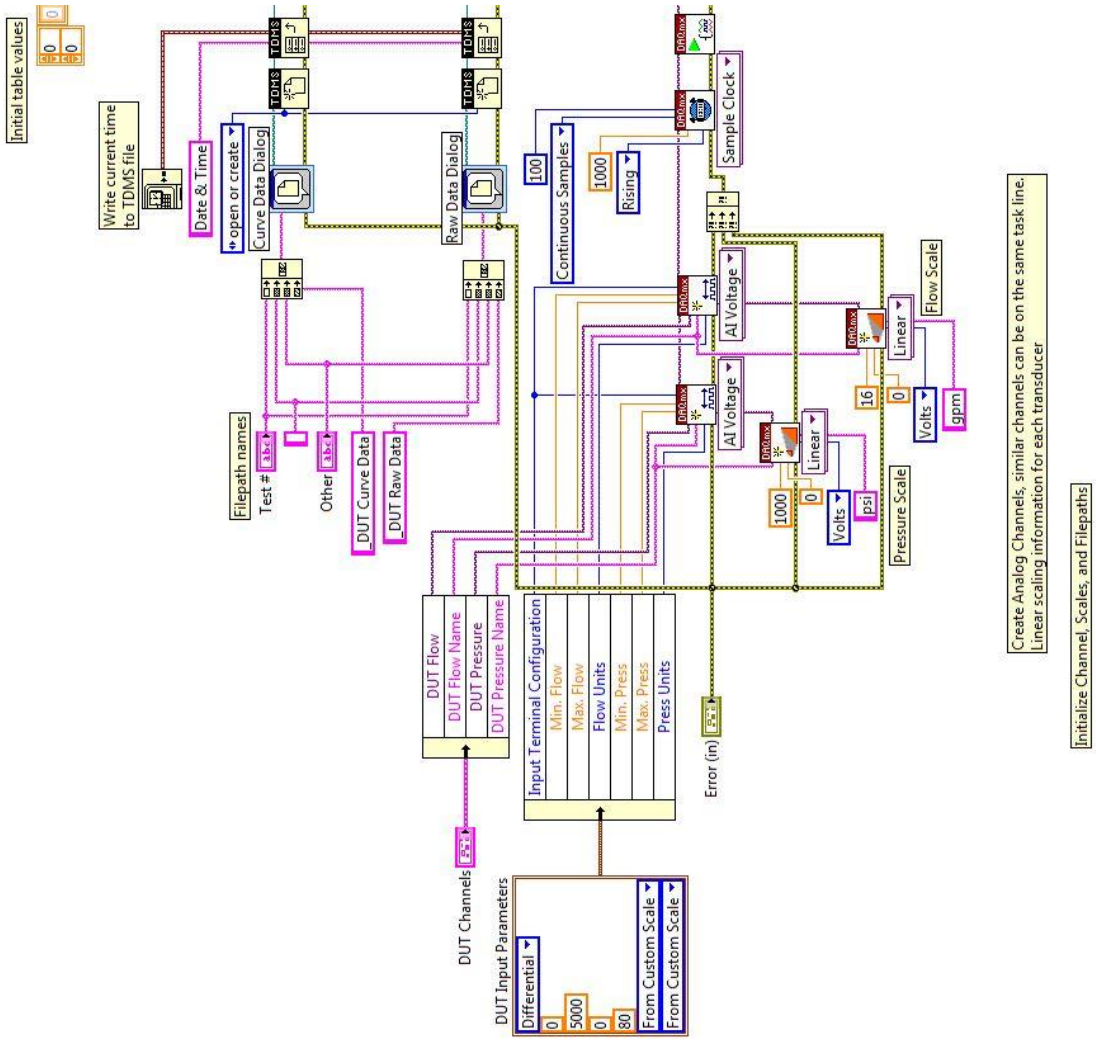

Figure 8.1: Block Diagram of hydraulic LabVIEW program. Illustrates how channels are created and initialized.

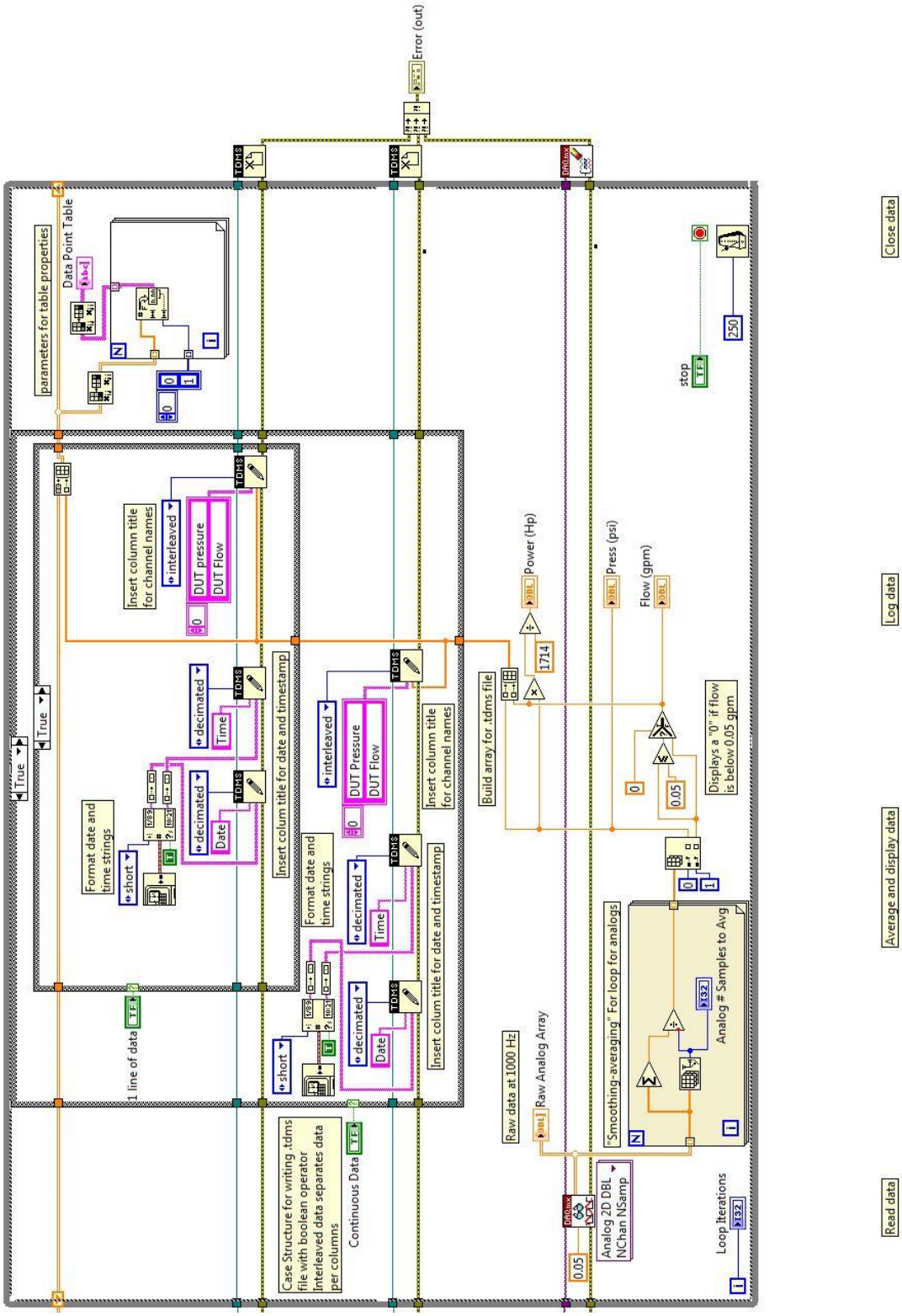

Figure 8.2: Block Diagram of hydraulic LabVIEW program. Illustrates the reading and logging of the data.

8.2 APPENDIX B – LABVIEW DRAWBAR BLOCK DIAGRAM

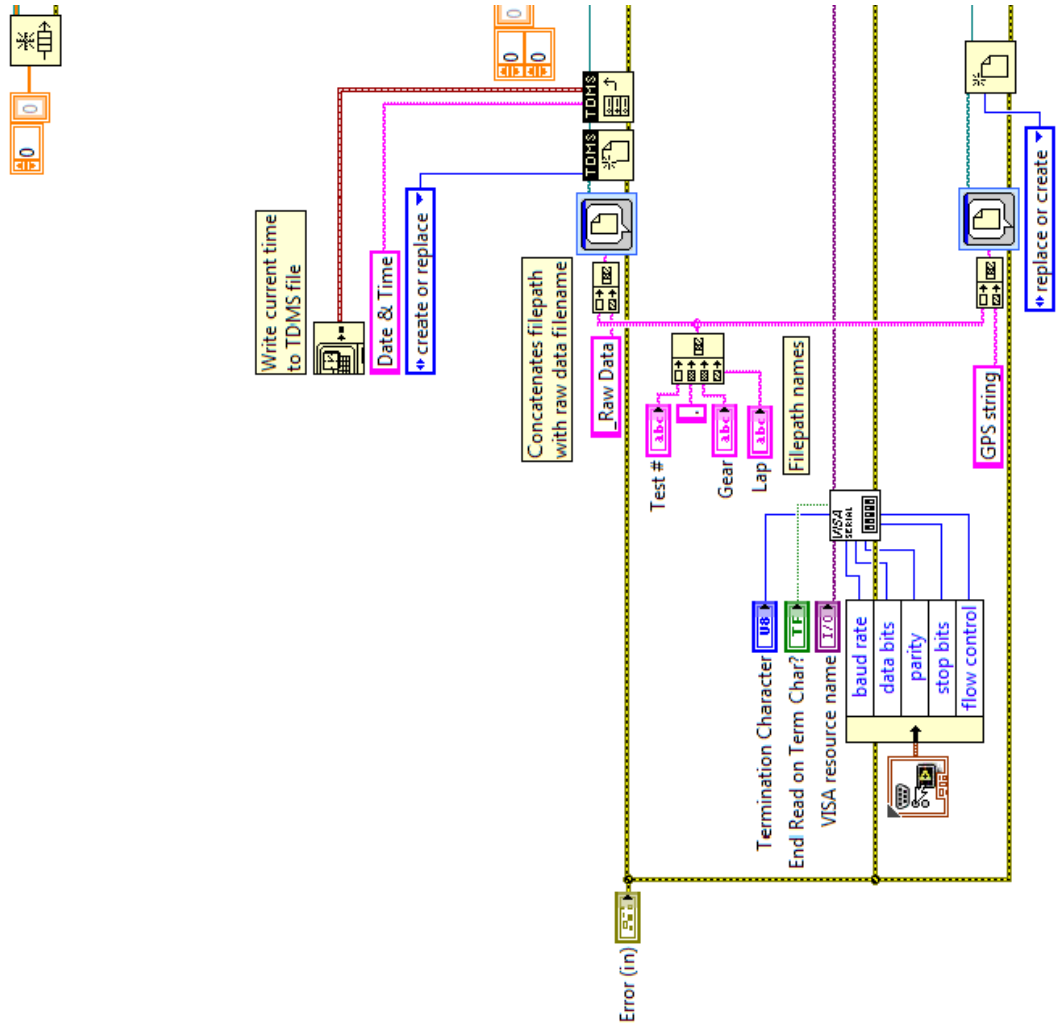

Figure 8.3. Block Diagram of drawbar LabVIEW program. Illustrates dialogue and file path names, and how the serial resource is initialized.

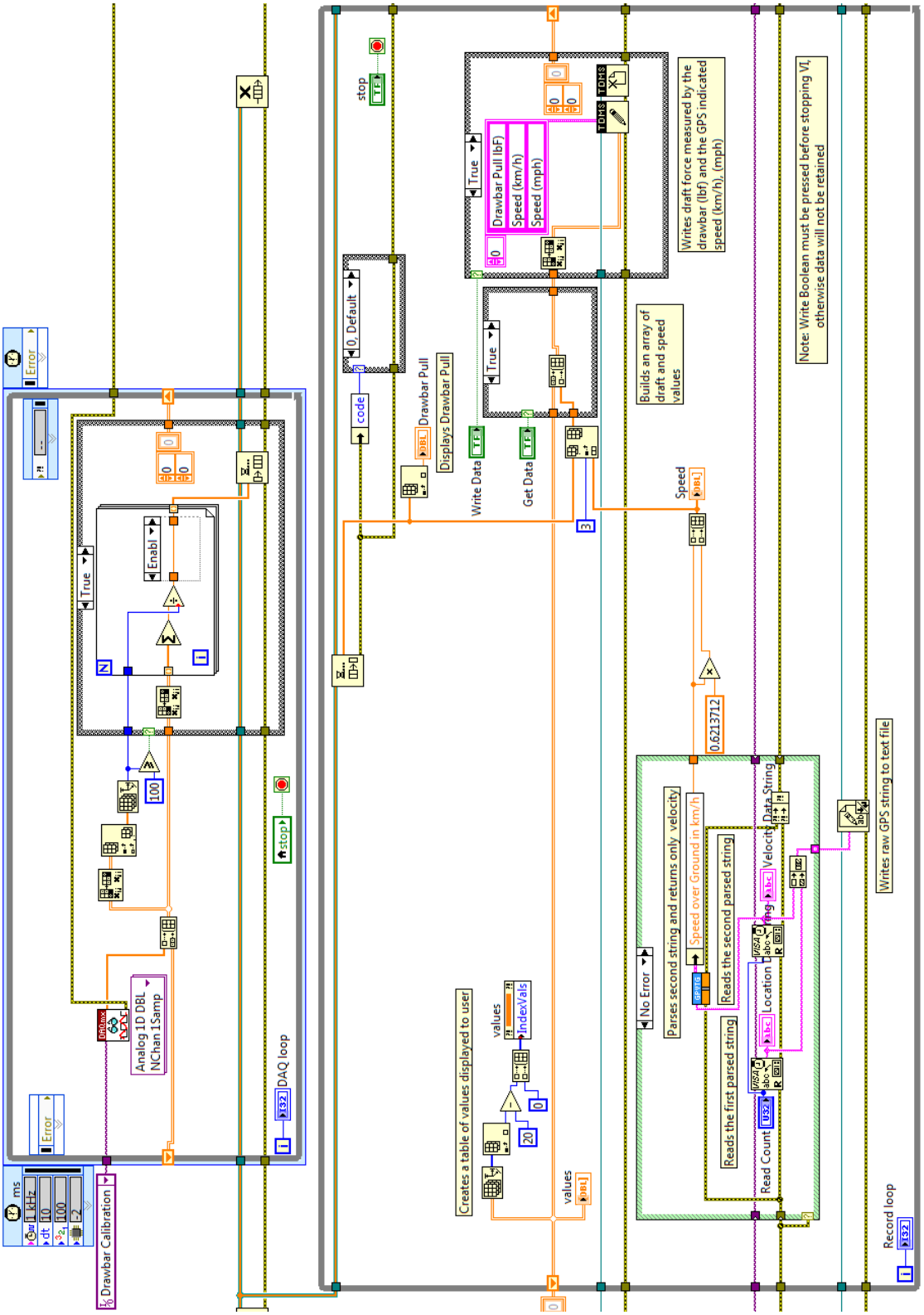

Figure 8.4. Block Diagram of drawbar LabVIEW program. Illustrates the reading and logging of the data.

8.3 APPENDIX C – LABVIEW PTO BLOCK DIAGRAM

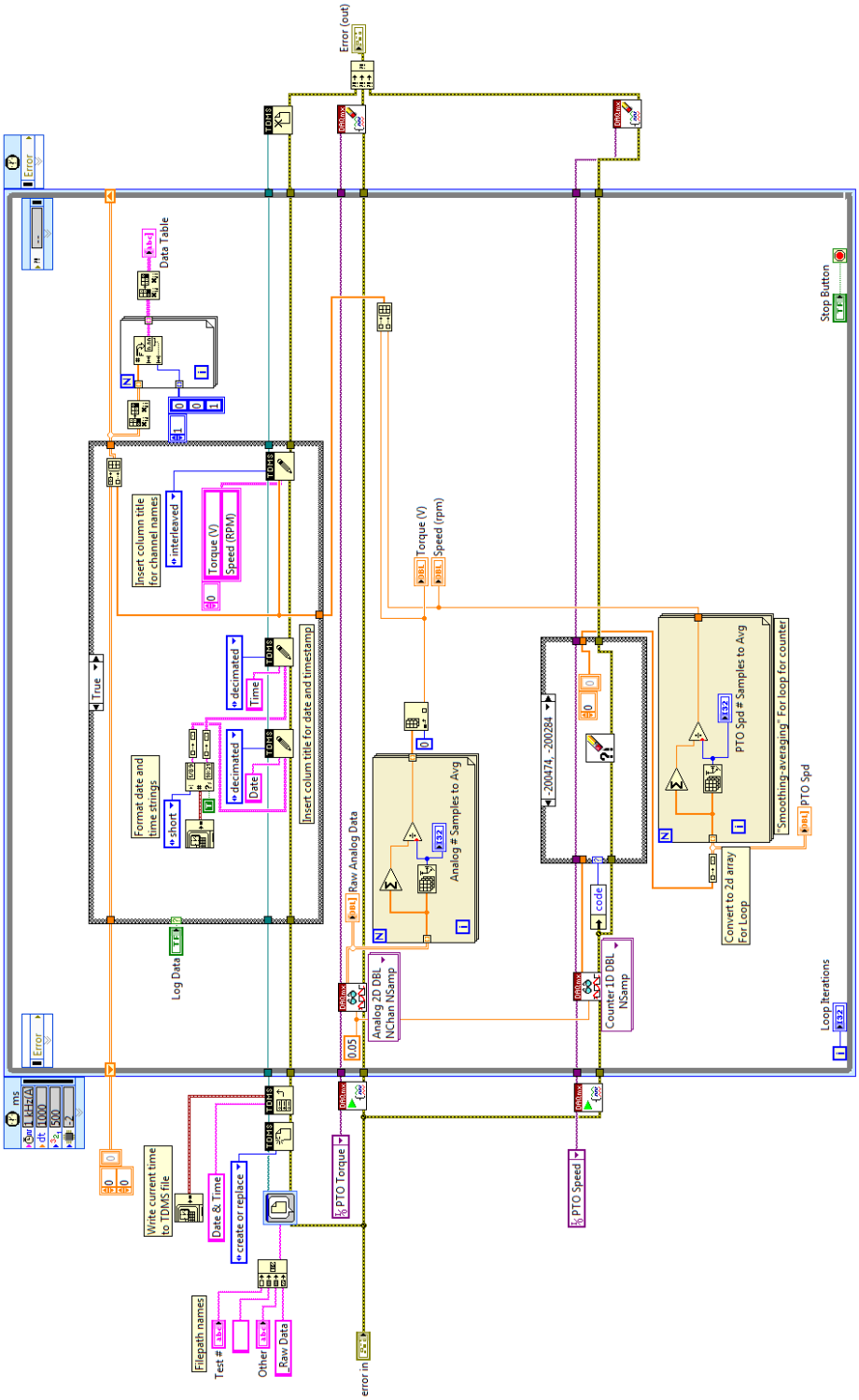

Figure 8.5. Block Diagram of PTO LabVIEW program. Illustrates the initialization, reading, logging, and termination functions of the VI.